LAPPEENRANTA UNIVERSITY OF TECHNOLOGY
School of Technology
Energy Technology

Maria Fedorovicheva

MODELING OF TEMPERATURE REGIMES IN A FURNACE OF BUBBLING FLUIDIZED BED BOILER

Examiners: Professor, D.Sc. (Tech.) Esa Vakkilainen
Docent, D.Sc. (Tech.) Juha Kaikko

ABSTRACT

Lappeenranta University of Technology
School of Technology
Master's Degree Program in Energy Technology

Maria Fedorovicheva

Modeling of temperature regimes in a furnace of bubbling fluidized bed boiler

Master's Thesis

2014

82 pages, 19 pictures, 13 tables

Examiners: Professor, D.Sc. (Tech.) Esa Vakkilainen
Docent, D.Sc. (Tech.) Juha Kaikko

Keywords: solid biofuels, combustion, bubbling fluidized bed boiler, heat transfer, modeling, temperature profile.

The work is mainly focused on the technology of bubbling fluidized bed combustion. Heat transfer and hydrodynamics of the process were examined in the work in detail. Special emphasis was placed on the process of heat exchange in a freeboard zone of bubbling fluidized bed boiler.

Operating mode of bubbling fluidized bed boiler depends on many parameters. To assess the influence of some parameters on a temperature regime inside the furnace a simplified method of zonal modeling was used in the work. Thus, effects of bed material fineness, excess air ratio and changes in boiler load were studied.

Besides the technology of combustion in bubbling fluidized bed, other common technologies of solid fuels combustion were reviewed. In addition, brief survey of most widely used types of solid fuel was performed in the work.

ACKNOWLEDGMENTS

This thesis was written as a part of the Master's program at Lappeenranta University of Technology.

I would like to express my gratitude to Professor Esa Vakkilainen for his guidance during the master's thesis preparation and also for the opportunity to take part in the Double degree program between Lappeenranta University of Technology and Moscow Power Engineering Institute.

TABLE OF CONTENTS

NOMENCLATURE

A_b	bed surface area	m^2
A_F	furnace cross section area	m^2
A_p	total surface of particles in the bed	m^2
a_f	entrainment constant	1/m
a_1	approximated coefficient	
b_1	approximated coefficient	
C_D	drag coefficient	
c_{pa}	air specific heat at constant pressure	kJ/kg·K
c_{pash}	ash specific heat at constant pressure	kJ/kg·K
c_{pf}	fuel specific heat at constant pressure	kJ/kg·K
c_{pfg}	flue gases specific heat at constant pressure	kJ/kg·K
c_{ps}	sorbent specific heat at constant pressure	kJ/kg·K
C_1	tube wall thickness amendment	mm
C_2	tube wall corrosion amendment	mm
D_b	bed diameter	m
D_h	hydraulic diameter	m
d_p	particle diameter	m
d_{pi}	particle diameter of the fraction i	m
d_{to}	outage tube diameter	m
e	mathematical constant, base of the natural logarithm	2.7183
F_A	Archimedes force	N
F_D	Drag force	N
F_G	Gravity force	N

g	acceleration of gravity	9.81 m/s^2
h	height, longitudinal coordinate	m
H_b	bed height	m
H_{FB}	freeboard height	m
h_{fwi}	feed water inlet enthalpy	kJ/kg
h_{fwo}	feed water outlet enthalpy	kJ/kg
h_i	input enthalpy of water	kJ/kg
H_{mf}	bed height at minimum fluidization	m
h_{ss}	enthalpy of saturated steam	kJ/kg
h_{ssh}	superheated steam enthalpy	kJ/kg
h_{ws}	enthalpy of saturated water	kJ/kg
L	distance	m
L_b	mean beam length	m
L_{max}	maximum distance from distribution grate at which gas temperature becomes equal to bed temperature	m
M_a	air molar mass	g/mole
m_a	air rate	kg/s
m'_a	amount of air per 1 kg of fired fuel	kg/kg
m_{ap}	primary air rate	kg/s
m_b	mass of bed	kg
m_{bd}	blowdown water flow	kg/s
m_{ds}	desuperheating water flow	kg/s
m_f	fuel feed rate	kg/s
m_{fg}	flue gases rate	kg/s
m'_{fg}	amount of flue gas per 1 kg of burned fuel	kg/kg

m_{fw}	feed water rate	kg/s
M_g	gas molar mass	g/mole
m_{im}	mass of inert bed material	kg
m_{ms}	main steam rate	kg/s
m_s	sorbent feed rate	kg/s
M_s	sorbent molar mass	g/mole
n'_a	amount of air for combustion of 1 kg of fuel	mole/1 kg of fuel
n_i	mass fraction of particles with diameter d_{pi}	
p	maximal admissible working pressure	Pa
Δp_b	pressure drop in a bed	Pa
Q_{ap}	air preheating heat demand	W
Q_{api}	heat coming to the bed with primary air	W
Q_b	heat released in bed	W
Q_{bl}	heat losses through bed lining	W
Q_{br}	heat radiated by bed surface	W
Q_c	combustion heat rate	W
q_{cs}	cross section heat load	W/m^2
Q_d	heat losses with drained ash	W
Q_{eco}	economizer heat demand	W
Q_{ev}	evaporative heat demand	W
Q_{fg}	heat loss with flue gases	W
Q_{fi}	physical heat of incoming fuel	W
Q_{sh}	superheater heat demand	W
Q_{tot}	total heat demand for steam generation process	W
r	heat of vaporization	kJ/kg

R_l	thermal resistance of lining	$m^2 \cdot K /W$
r_o	radius of the orifice on distribution grate	m
t_a	ambient temperature	°C
t_{ai}	incoming air temperature	°C
t_{ap}	temperature of preheated air	°C
t_b	average bed temperature	°C
T_b	average bed temperature	K
T_{fb}	average freeboard temperature	K
T_o	gas temperature at orifice on distribution grate	K
T_s	heat transfer surface temperature	K
t_{tw}	temperature of wall tubes surface	°C
t_{ws}	temperature of saturated water	°C
U_f	superficial fluid velocity	m/s
U_{mf}	minimum fluidization velocity	m/s
U_o	gas velocity in orifice on distribution grate	m/s
U_p	single particle velocity	m/s
U_t	transport velocity	m/s
U_w	wind velocity	m/s
V_b	bed volume	m^3
V_F	furnace volume	m^3
V_p	single particle volume	m^3
V_ε	voids volume	m^3
X_a	air excess coefficient	
x_d	share of ash drained from the bed	
X_b	bed combustion fraction	

X	combustion fraction

Dimensionless numbers

Ar	Archimedes number
Ga	Galilei number
Nu	Nusselt number
Nu_b	Nusselt number for a bed
Re	Reynolds number
Re_{mf}	Reynolds at minimum fluidization
Re_p	Reynolds number for fluidized bed particle
Re_t	Reynolds number terminal (transport)

Greek symbols

α	total heat transfer coefficient	$Wt/m^2 \cdot K$
α_e	external heat transfer coefficient	$Wt/m^2 \cdot K$
α_{gc}	heat transfer coefficient for emulsion gas convection	$Wt/m^2 \cdot K$
α_{gp}	gas-particle heat transfer coefficient for whole bed	$Wt/m^2 \cdot K$
α_{pc}	particle convection heat transfer coefficient	$Wt/m^2 \cdot K$
α_{rad}	radiation heat transfer coefficient	$Wt/m^2 \cdot K$
α_{ws}	heat transfer coefficient to water/steam mixture	$Wt/m^2 \cdot K$
δ_{tw}	tube wall thickness	m
ε	void fraction of the bed (porosity)	
ε_b	emissivity of the bed surface	
ε_{bs}	generalized emissivity of the system fluidized bed-immersed surface, including view factor	

ε_g	emissivity of the gas	
ε_m	emissivity of the gas-particle mixture in the furnace	
ε_{mf}	bed voidage at minimum fluidization	
ε_p	emissivity of the particles in the bed	
ε_s	emissivity of heat transfer surface	
η_B	total efficiency of steam generation	%
λ	friction factor	
λ_g	gas thermal conductivity	Wt/m·K
λ_{tw}	tube wall thermal conductivity	Wt/m·K
μ_f	dynamic viscosity of fluid	Pa·s
ν	material strength factor	
ν_f	kinematic viscosity of fluid	m^2/s
π	Pi number	3.14159
ρ_b	bulk density of a fixed bed	kg/m^3
ρ_f	density of fluid	kg/m^3
ρ_{fb}	bulk density of a fluidized bed	kg/m^3
ρ_m	emulsion density	kg/m^3
ρ_p	single particle density	kg/m^3
ρ_0	fluidized bed density just above the bed surface	kg/m^3
ρ_∞	emulsion density above transport disengaging height	kg/m^3
ϕ_s	particle sphericity	
σ	Stefan-Boltzman constant	$5.67 \cdot 10^{-8}$ $W/m^2 \cdot K^4$
σ_l	material strength	Pa
ω_a	fuel ash content	
ω_f	fuel mass share in the bed	

ω_H	reactive hydrogen mass share in the 1 kg of fuel	
ω_S	sulphur mass share in the fuel	
ω_{wf}	fuel moisture content (mass share)	
ω'_{wf}	total moisture content (with combustion products)	
ω_{ws}	sorbent moisture content (mass share)	

Abbreviations

BFB	bubbling fluidized bed	
CFB	circulating fluidized bed	
HHV	higher heating value	MJ/kg
LHV	lower heating value	MJ/kg
TDH	transport disengaging height	m

1. INTRODUCTION

According to the data of International Energy Agency for 2011, more than 40% of energy in the world is produced by combustion of solid fuels, mainly coal and peat. The share of primary solid biofuels in the total electricity and heat production is about 1.4% (4% in Europe) and continues to grow **[1]**. It can be explained, first of all, by increase of fossil fuel prices on the international market and global policy to reduce carbon dioxide emissions.

Wide use of solid fuels and interest associated with energy production from biofuels such as wood, sawdust, wood chips and other industrial and agricultural waste cause development of solid fuel combustion technologies. Currently, there are three the most commonly used technologies of solid biofuel combustion: grate firing, bubbling fluidized bed (BFB) firing and circulating fluidized bed (CFB) firing. All the technologies have their own advantages and disadvantages that are discussed later in this paper.

Combustion technology and type of fuel determine boiler design and operational conditions. The previous years' experience allows to improve methods of fuel combustion greatly. For updating of boiler functioning and modernization of its single parts modeling is often used in practice. Modeling is can be applied for prediction of operational conditions during different boiler regimes such as starting-up and adjustment, regular regime and stoppage. Influence of change in fuel feed or fuel quality (increase of moisture content, for example), variation of excess air ratio also can be simulated.

It is to be noted that modeling has a significant importance for large-scale projects such as steam boilers because of complexity and expensiveness of the real experiments. It allows to optimize operational conditions for running objects when it is impossible to carry out any experiments without negative impact on production or equipment.

Modeling process can be simplified, focused on individual process inside the object or can simulate the object completely. There are many models of varying complexity for boilers nowadays: the most difficult and detailed fluid dynamic models which represent the information about temperature, pressure and concentration fields in three dimensions; more simplified fluidization models which allow to get gaseous and solid species profiles as well as temperature distribution; black box models which give only overall heat and mass balance of the boiler **[24]**.

The main aim of the present work is to develop a simplified one-dimensional model applicable for studying of heat exchange processes inside the furnace of bubbling fluidized bed boiler. There is a lack of experimental information about heat transfer in furnaces of industrial boilers using this method of combustion. So, the model can be useful for comprehension of heat transfer process as well as mechanism of fluidization on which principle of BFB boiler operation is based.

Influence of different parameters (such as bed material fineness, excess air ratio, boiler load) on heat transfer process and particularly on temperature distribution in the furnace of bubbling fluidized bed boiler is under consideration in this work.

2. TYPES OF SOLID FUEL FIRED BOILERS.

In this section main aspects of solid fuel combustion are briefly reviewed. Way of combustion and type of fuel determine processes occurring inside combustion chamber. Combustion technology has a strong influence on a mechanism of heat transfer to surfaces and overall thermal efficiency of the process.

2.1. Grate boilers.

Grate firing is the oldest method of solid fuels firing. At the beginning of the 20th century, grate firing was the only available combustion technology for coal. Nowadays it is used mainly for combustion of biomass and waste. It is old, but proven, reliable and cost-effective technology. The common capacity range of grate boilers is from 0.3 up to 150 MW_{th} in industry and CHP. **[4]**

The technology is based on a fuel feeding onto a grate where combustion occurs. The way of fuel feeding and the type of grate depend on the fuel properties.

Thus, *travelling grate* is commonly used for coal combustion. Coal is fed from metering bin to a forward moving steel grate (velocity varies from 1.5 to 15 m/h) and forms a layer 10–30 cm thick, which goes through the stages of heating, drying, ignition and burning at the temperature about 1200℃. The ash is removed at the end of the grate. The major part of the combustion air is blown from underneath of the grate for efficient contact with the fuel and cooling the grate at the same time. The height of fuel layer depends on the combustion characteristics of fuel such as volatile matter content and fuel granularity. Good burnout is assured by sufficient residence times for the solid fuel on the grate and for the gases in the furnace. Fuel layer height, grate velocity and burning rate should be coordinated in order to exclude unburnt fuel and gases above the devolatilisation zone.

The other way of feeding – spreader stoker – is used for fuel contains fine particles. Spreader stoker realizes a combination of suspension firing and grate firing, when the fuel is fed into the furnace above a burning layer of coal. Fine particles are burned in suspension and coarse particles fall to the moving grate. This method of combustion may increase the grate heat load by 50% compared to the previous one. The main disadvantage of spreader stokers is high percent of fuel carried out of the furnace, so recirculating system is needed.

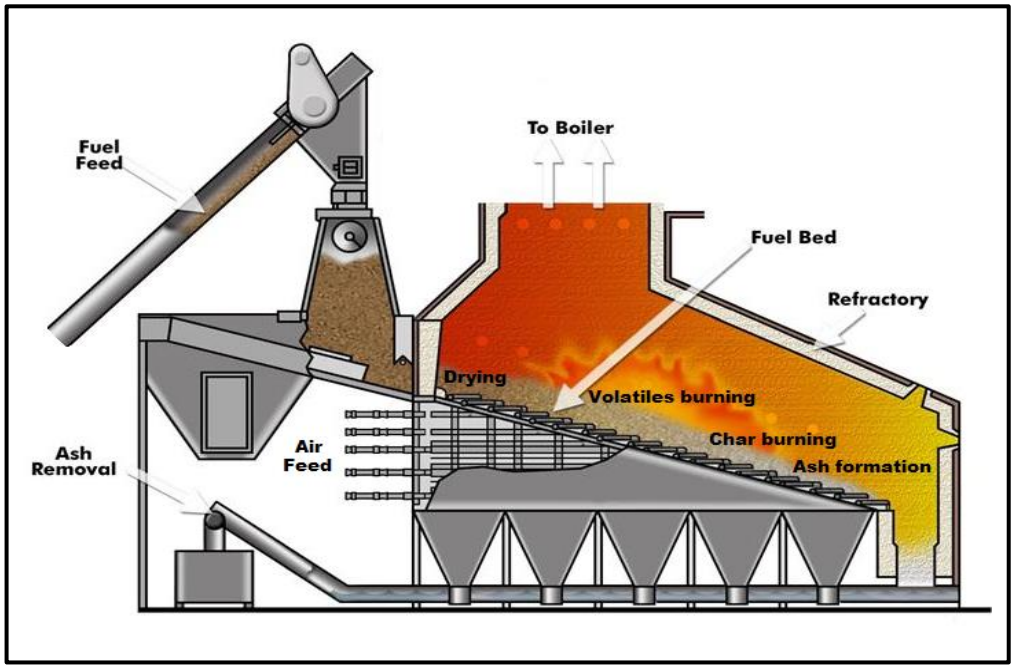

Fig. 1. Boiler furnace with modern mechanical grate. Source: Wellons FEI Corp.

For fuel with high ash content and low calorific value travelling grate isn't appropriate. Problems, concerned with ignition and combustion process, can be solved by use of *reciprocating grate*. Fig. 1 shows a schematic arrangement of furnace equipped such grate. Operating principle of the reciprocating grate is continuous poking and raking of the fuel in order to ensure better air and radiant heat access to the fuel as well as sintering prevention. Fixed and moving rows of grate are alternate with each other. Fuel is pushed by moving rows and burns during its transportation. The heat load of reciprocating grate is about 1 MW/m^2 **[4]**.

The other commonly used type of grate – *vibrating grate* – designed mainly for combustion of biomass and multi-fuels with little or almost no ash content and calorific value above 20 MJ/kg. Vibrating grate has quite simple mechanical design with few movable parts. It consists of air- or water-cooled bars attached to inclined vibrating frames. The primary combustion air is fed through air slots between bars. Fuel is transported from the top of grate by short vibrating movements repeated after definite time interval. Frequency of vibration depends on fuel properties and combustion conditions. When suitable fuel types are used grate heat load may be up to 1.5 MW/m^2.

Fuel types with large particle variations (excluding fuels with fine fraction) and moisture contents ranging from 10% up to 60% can be successfully fired in grate boilers. Grate firing systems are not prone to bed agglomerations and provide very good performance burning high alkali content fuels such as straw, corn cobs, agro crops and poultry litter **[7]**.

2.2. Bubbling fluidized bed boilers.

The technology of fluidized bed firing was introduced for the first time in 1921 by German chemist F. Winkler, who applied it for coal gasification. Development of bubbling fluidized bed (BFB) technology for fuel combustion began later, in 1960s. First commercial BFB boiler was with capacity 20 MW_{th} and nowadays capacity of this boiler type may reach 350 MW_{el} (Takehara power plant in Japan, started up in 1995). BFB technology demonstrates a high efficiency of the combustion process.

The term “fluidized bed” describes a mixture of particulate solids and gas placed under specific conditions, when it behaves itself as a fluid. The principle of fluidized bed combustion technology is that fuel burns in the hot bed of noncombustible inert material fluidized by upward air flow. At a certain air velocity, bubbles start to appear in the bed and it behaves like a boiling liquid.

Force of air flow keeps solid particles floating, but it's not enough to carry them out of the bed.

As to the inert material forming the bed, it is a mass of solid particles with size range from 0.1 to 1.0 mm. Usually it is sand or gravel. Biomass-fired boilers may use also special bed materials including synthetics to avoid agglomeration in the bed. Size of bed material particles is not necessary defined by fuel particles size, because fuel constituent in the bed is only from 1 to 3% **[2]**. However, fuels with high ash content influence on both size and composition of the bed materials.

A typical BFB boiler (fig. 2) is composed from a furnace and a convective heat exchange section. The furnace includes a bed with sand and a freeboard above it. Solid fuels are crushed in a crusher to the size 6–1 mm and then transported to the boiler. Limestone is admixed to the fuel with high sulphur content for desulphurization. Two ways of fuel feed are possible: over-bed (for coarse fuel) or below the bed (fine fuels) surface. The primary air enters the bed through nozzles of a bottom grate, which assures uniform air distribution.

Suspended fuel particles burn in a hot fluidized bed of ash, sand and limestone. Continuous mixing of solid particles and gas promotes conditions for intensive heat transfer and chemical reactions during combustion. Bubble eruptions provide release of solid particles to the freeboard. Contact of particles with wall tubes and other surfaces increases heat transfer as well. Volatiles and char particles in the freeboard burn in the secondary air, blown through the walls of furnace.

BFB boiler is applicable to low-grade solid fuels combustion, including most types of coal and woody biomass, at high efficiency and without of expensive fuel preparation. The temperature of fluidized bed is typically around 800–900 °C. The lower limit is defined by combustion reactivity of fuel and the upper limit is defined by ash sintering temperature to eliminate formation of agglomerations in the bed and slagging of heat transfer surfaces. In the freeboard space combustion temperature can achieve 1200°C (NO_x intensive formation starts at about 1300°C).

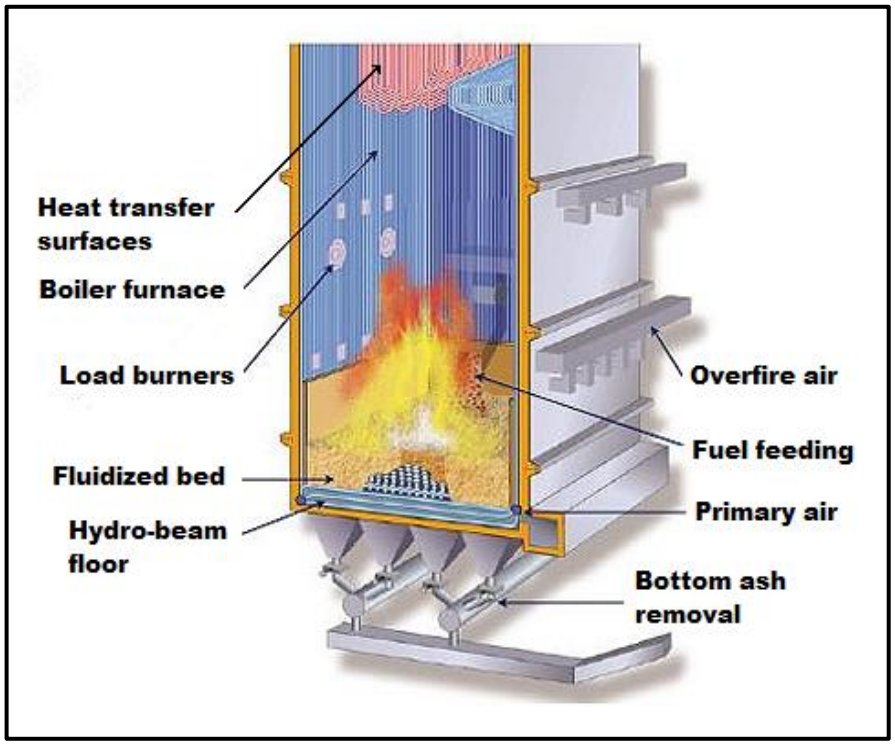

Fig. 2. Bubbling fluidized bed furnace. Source: power-technology.com.

High alkali content fuels (such as straw, agro crops, poultry litter) are difficult for combustion in fluidized bed boilers due to high agglomeration tendency. The organic alkalis in the fuel vaporize at high bed temperatures, interact with other fuel components or inert bed material (silica) and produce low melting compounds that can cause eutectics formation and heat transfer surfaces fouling **[8]**. Fouling of heat transfer surfaces is associated mainly with high potassium content in the fuel, while in-bed agglomeration formation depends mainly on sodium content **[6]**. Agglomerations in fluidized bed lead to uneven fluidization regime, possible defluidization and interruption of boiler operation.

2.3. Circulating fluidized bed boilers.

At the end of the 1970s, circulating fluidized bed (CFB) method of combustion was developed as an alternation to bubbling fluidized beds and has replaced them

more and more since. For 30 years possible CFB boiler capacity increased from few MW_{th} to 460 MW_{el} (Lagisza power plant in Poland, started up in 2006).

In CFB boilers, gas velocity is higher than in BFB boilers and the inert bed material is in the fast fluidization regime: great quantity of solid particles are carried out of the furnace. There is no definite fluidized bed with a high density of particles. Solid constituent gradually decreases with the height. Particle mixing is very intensive.

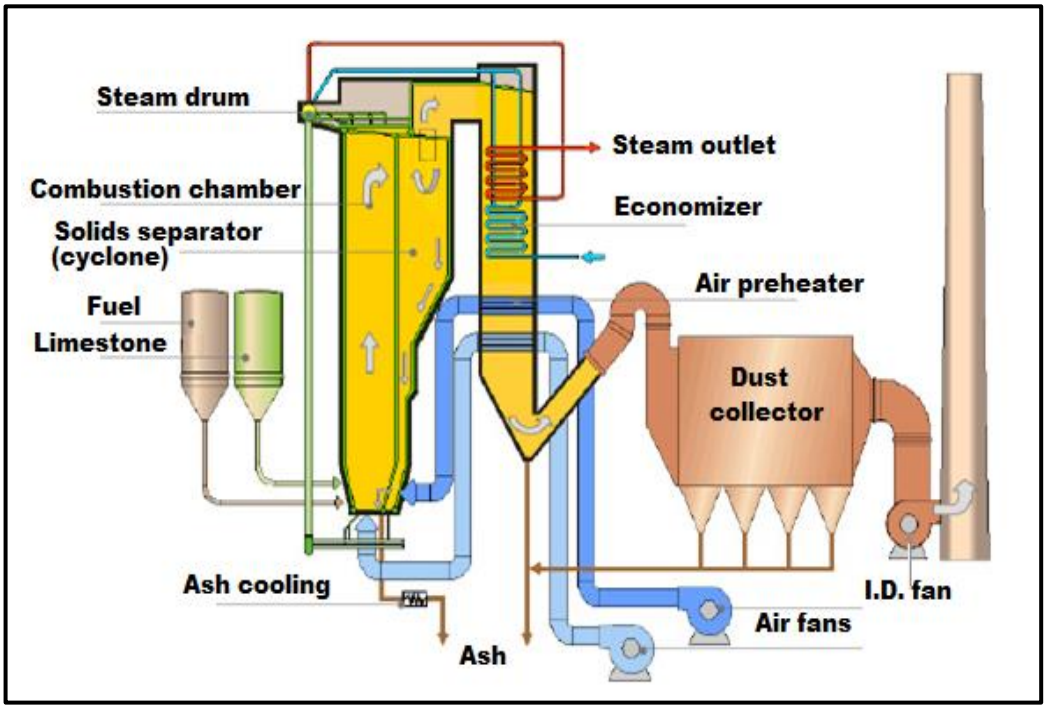

Fig. 3. The arrangement of circulating fluidized bed boiler with integrated cyclone. Source: Foster Wheeler Europe.

The fluidizing velocity is one of the main characteristics of the process. Its value defines bed cross-sectional area and other design parameters. So, high air velocity allows to build more compact boilers with cross-sectional heat load about 6 MW/m^2. But it also leads to increase of the boiler height for ensuring a sufficient particle residence time for combustion process and desulphurization. Higher fluidizing velocities also accelerate erosion of internal surfaces and require powerful fans.

In CFB boilers (fig. 3) combustion takes place in the whole volume of the vertical chamber, which is characterized by small cross section and considerable height. The walls of the chamber are covered with water tubes and its lower part, where erosion process is most intensive, is protected by fire bricks. The temperature of fuel combustion in CFB boiler is about 800–900°C. Intensive mixing of fuel particles and air, frequent contact of solids with each other and with heat transfer surfaces provide very good conditions for the fuel combustion and intensive heat exchange. Unburned fuel particles and inert material are separated from flue gases by cyclone and fed back into the lower part of the fluidized bed by a special duct. The system of fuel particles recirculation provides fuel combustion with efficiency about 99.5%.

CFB boilers have unmatched fuel flexibility. Types of fuel with high moisture content (up to 70%) and low calorific value can be successfully burnt there. The diversity of fuels ranges from conventional (coal of various carbonization, petroleum products, peat) to alternative (wood residues, municipal wastes, agricultural and industrial wastes, sludge).

2.4. Pulverized fuel fired boilers.

Pulverized way of combustion is typical for coal. This technology was introduced in 1911. Since then it has been well developed and nowadays applied on more than 90% of coal-fired power station boilers **[5]**. The unit power of these boilers approaches 2000 MW_{th}.

Technology is based on injection of pulverized fuel and primary air mixture to the furnace volume through the system of nozzles. Combustion process takes place at temperatures about 1300–1700°C (depends on fuel type). Particle residence time in the combustion chamber is typically from 2 to 5 seconds, so fuel particle size must be small enough to burn out during this period of time **[4]**. Efficiency of the fuel combustion depends strongly on grinding degree of fuel. Commonly pulverized fuel fired boilers have very high combustion efficiency (may achieve

99.0– 99.5%). There is no intensifying inert material in the furnace of this boiler type as well as recirculation system, and fuel particles burns up in a single pass through the furnace. The combustion process may be accelerated by use of finely pulverized fuel, swirl burners and increase of combustion air temperature. Cross section heat load in this case can reach 6–7 MW/m^2.

Pulverized fuel firing requires fuel preparation with stages of drying and grinding. Fuel is ground usually to the size of 300–75 microns. Such small size of particles excludes losses with unburnt fuel. It allows to burn solid fuels almost as easily and efficiently as a gaseous fuel.

As was mentioned above, the most commonly used type of fuel for pulverized firing is coal. Almost all coal types, from anthracite to lignite coal, can be combusted using this technology. Biomass and other materials can also be pulverized and admixed to coal powder. One of the main advantages of pulverized fuel firing is flexibility to varying fuel quality.

2.5. Comparison of boiler types.

Previously the most commonly used technologies of solid fuel combustion were reviewed. They all have advantages and disadvantages determining their prevalence in the global power industry. Primary physical characteristics of different types of boiler are compared in tab. 1.

One of the main characteristics for boiler is combustion efficiency. It is affected by the heat losses due to carryover of unburned char particles in fly ash to a greater extent and by chemically incomplete fuel combustion to a lesser extent. The most efficient combustion process is in pulverized fuel firing boilers (about 99%): small size of fuel particles and total mixing with air almost exclude incomplete burning. The combustion efficiency of a CFB boiler is in the range of 97.5 to 99.5%, while that for a bubbling bed is lower, in the range of 90 to 96%. High combustion efficiency of fluidized bed boilers can be explained by good

gas–solid mixing and high burning rate (even for coarse fuel particles). Grate boilers have the lowest combustion efficiency (85–90%) due to relatively bad fuel–air contact and low intensity of mixing.

Tab. 1. Comparison of physical features of fluidized bed boilers with those of other types **[2]**.

Characteristics	Stoker	Bubbling	Circulating	Pulverized
Height of bed or fuel burning zone, m	0.2	1–2	10–30	27–45
Superficial gas velocity (average in a cross-section), m/s	1–2	1.5–2.5	3–5	4–6
Excess air, %	20–30	20–25	10–20	15–30
Grate heat release rate, MW/m^2	0.5–1.5	0.5–1.5	3.0–4.5	4–6
Coal size, mm	32–6	6–0	6–0	<0.1
Turn down ratio (fuel load variation)	4:1	3:1	3–4:1	3:1
Combustion efficiency, %	85–90	90–96	95–99.5	99–99.5
Nitrogen oxides, ppm	400–600	300–400	50–200	400–600
Sulfur dioxide capture in furnace, %	None	80–90	80–90	None

Cross-section heat load (grate heat release rate) characterizes compactness of boiler. It shows how much energy can be produced by 1 m^2 of furnace area. Pulverized fuel fired and CFB boilers have the highest rates because of combustion in the whole furnace volume (6 and 4.5 MW/m^2 accordingly). And the height of bed or fuel burning zone (tab. 1) also explains it.

Pulverized fuel firing technology has many advantages, but it requires more fuel preparation than fluidized bed boilers and especially grate boilers, where fuel particles of relatively large size (tab. 1) can be burnt without preliminary drying and grinding stages.

Global heat and electricity production industry is responsible for more than 30% of greenhouse gas emissions **[6]**, thus environmental aspect of fuel combustion is very important, when different boiler types are compared.

Fluidized bed combustion technology, according to values presented in table 1, has significant advantages in relation to other technologies. Thus, CFB boilers have the lowest nitrogen oxides emission that can be explained by relatively low temperatures in the combustion chamber (about 900°C). Nitrogen oxides can be formed from nitrogen in fuel or molecular nitrogen in the combustion air. The principal nitrogen pollutants generated by boilers are nitric oxide NO and nitrogen dioxide NO_2, collectively denoted as NO_x. NO has the largest share among nitrogen oxides produced during combustion (about 95%). NO formation is not intensive below 1000 °C and also at low excess air (CFB boilers have the lowest one in comparison to other boilers, tab. 1).

As to the sulphur dioxide (SO_2) capture, fluidized bed boilers also have advantages in comparison with other boiler types. In fluidized bed boilers SO_2 is removed during the combustion process by adding limestone ($CaCO_3$) into the bed. Harmful sulphur dioxide is then converted into an inert solid material $CaSO_4$. This technology allows to reduce investment costs because there no special devices for flue gas desulphurization is needed.

Grate boilers and pulverized fuel fired boilers don’t comply with environmental requirements for SO_2 and NO_x emission without usage of very expensive (relatively to the price of the boiler) equipment for flue gas cleaning.

3. TYPES OF SOLID FUEL AND FUNDAMENTALS OF COMBUSTION IN FLUIDIZED BED.

In this section the most widely used types of solid fuel and fundamentals of combustion are briefly reviewed. Detailed consideration of a fuel combustion mechanism leads to comprehension of processes occurring in a fire chamber. Fuel particles play a huge role in heat exchange with boiler heat transfer surfaces and that cannot be ignored.

3.1. Solid fuels.

Coal is the most-used fossil fuel in the world. It is about 40% of global energy produced from coal **[9]**. During the last years coal has been increasingly neglected for energy production due to its environmental compatibility. In many countries there is a tendency to reduction of coal share in heat production for district heating systems and electricity generation by large boiler units **[4]**.

Coal is a combustible black (most often) sedimentary rock usually occurring in rock strata in layers called coal beds or seams. Coal is a mixture of organic material and mineral matter (metals, their oxides and salts). The organic part is responsible for the energy content of the fuel, while the mineral part presents significant challenges in the design and operation of a boiler. Coal is composed primarily of carbon along with variable quantities of other elements, basically hydrogen, oxygen, sulfur and nitrogen (more detail in tab. 2). Coal types are commonly differentiated one from another according to ash and volatile content. So, the higher heating values (HHV) are also varied. HHV of coal is the largest amongst solid fuels (28 MJ/kg on average). But, as it was mentioned above, emissions from combustion are also quite high (tab. 3). Great content of sulphur and nitrogen enable coal combustion without subsequent process of SO_x and NO_x capture.

Countries with extensive coal resources endeavor to introduce new combustion technologies to decrease harmful emissions. Despite the fact that pulverized coal combustion has the highest efficiency (tab. 1), it is unacceptable from the ecological point of view. In this connection, technology of co-firing biomass with coal in pulverized boilers are introduced. It doesn't demands serious reconstruction, but significantly reduces SO_x, NO_x and dust emissions. Fluidized bed boilers, which are under a special attention in this work, can solve this problem better: more than 95% of the sulfur pollutants in coal can be captured inside the boiler by the sorbent and NO_x formation is decreased owing to low temperatures in the furnace.

Tab. 2. Composition of most widely used solid fuels (average values) **[10]**, **[11]**.

Fuel	**Dry ash-free matter basis**						**HHV, MJ/kg**	**Ash %**	**Moisture, %**
	Volatiles, %	**C,%**	**H,%**	**O,%**	**N,%**	**S,%**			
Coal	44–60	68–78	3.5-5.0	6–20	0.4-3.0	0.5	27–32	8–15	10–30
Peat	70	52–56	5.0-6.5	34	1.0-3.0	0.1–0.3	23.5	5–20	50
Wood	80	48–52	5.4-6.8	42–46	0.3-0.5	< 0.05	20	2	50-60
Bark	65	48–52	6.2-6.8	35	0.3-0.5	< 0.05	22	3	40–60
Sawdust	80	48–52	6.2-6.4	27	0.3-0.4	< 0.05	18	2	55
Straw	70	45–47	5.8-6.0	40	0.4-0.6	0.1–0.2	16	4	15–25

Tab. 3. Specific carbon dioxide emissions of most widely used solid fuels (average values) **[12]**, **[13]**.

Type of fuel	**Emissions in kg CO_2/kWh**
Coal	0.34
Peat	0.38
Wood	0.34
Bark	0.36
Sawdust	0.3
Straw	0.01

Peat is an accumulation of partially decomposed vegetation or organic matter. Peat forms in wetland conditions, where flooding obstructs flows of oxygen from the atmosphere. Peat has high carbon content (about 60%) and can be used as an alternative to coal in countries with extensive peat resources. Burning peat as a fuel instead of coal is better for the environment because it produces from 10% to 60% of the sulphur dioxide emissions that coal does and there is almost no mercury

Biofuel is renewable organic fuel, derived from living or recently living organisms. Bioenergy is produced from trees, crops, agricultural residues, animal wastes, organic municipal and industrial wastes. The share of primary solid biofuels in the global electricity and heat production is about 1.4%, and it rises from year to year due to its high availability and ecological compatibility. The most commonly used types of solid biofuel for combustion in boilers are wastes of woodworking industry (wood chips, sawdust) and agricultural biomass (including energy crops).

Compared to conventional fuels like coal and peat, biofuel combustion is accompanied by certain problems: biofuel quality depends on season and region, moisture content can reach 80%, fuel storing and feeding are more complicated, and fouling, slagging, and high-temperature corrosion are usual problems in biomass-fired boilers **[26]**.

The commonly used boiler types for biomass combustion are grate boilers and fluidized bed boilers. Biomass-fired BFB and CFB boilers may suffer from ash related problems to a greater extent: products of biofuel combustion can form compounds causing bed agglomerations and superheater corrosion.

According to ash composition, solid biofuels can be divided into some groups having significant differences in combustion properties. Woody fuels mainly belong to group with high potassium (K) and calcium (Ca) content in ash and herbaceous fuels belong to group with high silica (Si) and chlorine (Cl) ash content.

Wood biofuels have low content of nitrogen, sulphur and ash (tab. 2) compared to coal and peat. High moisture content of wood fuels (about 40–70%) considerably reduces fuel net calorific value. The composition of biofuel ash is strongly depends on the plant species, soil quality, weather conditions, harvesting time. As it was mentioned above, wood fuel ash is usually rich in calcium and potassium: CaO concentration in ash is about 30–50%, K_2O concentration is close to 10%. Ca and K form rich deposits on surfaces (CaO, $CaSO_4$ and K_2SO_4) that harden if not removed frequently by soot blowing. During combustion process K and Ca from biofuel ash can react with inert bed material component (SiO_2) and form viscid silicate layer onto the bed particles. It can lead to agglomerations and sintering of whole bed.

Bed agglomerations can be controlled by regularly discharging the bed ash and feeding fresh sand into the bed. It is possible to minimize sintering effect by decrease quartz content in the inert bed material or by replace it by less reactive olivine.

In general, the higher the fuel alkali and chlorine contents, the lower the sintering temperatures. Wood ash starts to sinter and form agglomerates between 900°C and 1000°C in combustion conditions. Coal and peat ashes are usually trouble free at these temperatures. Lower reactivity of coal and peat ashes is connected to a high content of quartz and various silicate-based minerals (aluminium silicates, calcium silicates, alkali silicates). Calcium and alkali in these minerals are not in free form like they are in biomass ashes. They are quite inert at the conditions of fluidized bed combustion. So it is a prevalent technology to co-fire coal or peat with biomass in multi-fuel fired boilers due to reduce agglomeration formation and sintering.

Herbaceous (agricultural) biofuels are very diverse by chemical composition and combustion properties. Cereal straws have relatively high potassium (K) and chlorine (Cl) contents. Grain husk and bagasse have very high SiO_2 contents in ash.

Straws have ash content about 5% (tab. 2). SiO_2 is the main ash component, but variations are quite large (60–70%), CaO share is about 4–14% and K_2O is 5–30%. The chlorine content in straws is high in comparison to wood biofuels (about 1–2%). It intensifies the fouling process and increases the risk of high temperature corrosion of superheaters.

The ash properties of cereal straws complicate the process of combustion in fluidized bed boilers. From the operational experience it is known that straw is a fuel with high fouling, slagging and corrosion properties. The sintering temperatures for this type of fuel are in the range 700–900ºC. Mechanism of agglomerations formation during straw combustion in fluidized bed boilers is different in comparison to wood biofuel combustion in the same boilers. In case of straw combustion sintering process is caused by molten ash inclusions consist on potassium chlorides and silicates as products of reactions between potassium, chlorine and silica present in large quantities in the ash. So, the composition of inert bed material does not have considerable influence on the sintering process in fluidized bed boilers utilizing fuels like cereal straw.

3.2. Details of fuel combustion process inside fluidized bed.

The fact that fuel cost forms a major part of operational costs of fluidized bed boiler, causes greater attention towards the efficiency of combustion process. Even 1% gain in the combustion efficiency can decrease operational costs considerably. Comprehension of the fuel combustion process plays a significant role in a rational boiler design.

As to the essence of the combustion process, it can be defined as an exothermic oxidation occurring at a relatively high temperature. During the process energy which is chemically bound in the fuel is converted into sensible heat. Combustion process depends strongly on fuel properties, heat and mass transfer intensity, hydrodynamic and thermodynamic parameters.

In fluidized beds combustion takes place at temperatures in the range of 800–900°C (in conventional boilers temperatures are much higher and reach 1000–1200°C). Uniform temperature field inside fluidized bed is provided by intensive particle mixing and good heat exchange between gas and solid particles. Solid fuel particles enter the fluidized bed and spread more or less uniformly throughout the volume owing to circulating movement of the bed material. Weight of injected solid fuel particles is from 0.5 to 5.0% by total weight of the fluidized bed. Other solids forming the bed – noncombustible inert material (sand, olivine), ash, limestone – constitute about 95–99.5% of bed weight. Continuous motion of fuel particles, their frequent collisions with particles of hot inert material and constant contact with air assure proper conditions for complete fuel combustion.

Coal is the most commonly used type of fuel for fluidized bed boilers. Coal can be co-fired with other fuels or be the only fuel. The combustion process of coal particles in the fluidized bed will be examined in this section in detail.

Solid coal particles in fluidized bed go through the typical stages of combustion: heating and drying, pyrolysis (devolatilization and volatile combustion), swelling and primary fragmentation, combustion of the residual char with secondary fragmentation and attrition. The dynamics of coal particles combustion inside the bed volume are shown particularly on fig. 4.

It is to be noted that oxygen distribution in the bed volume is not uniform. During combustion fuel particles use mainly oxygen available in the particulate phase. But the largest amount of air doesn’t take part in combustion process inside the bed. It passes the bed in bubbles and reacts with unburnt matter in freeboard zone.

Heating process starts at the moment when fuel particles enter the hot fluidized bed. Heat transfer coefficient between the inert material and fuel particles 5–10 mm in diameter at the temperature difference 800°C is about 300 $W/m^2 \cdot K$ **[3]**. Heating rate depends mainly on particle size and varies in a wide range (usually around 100°C/sec).

Owing to intense particle-to-particle heat transfer, the temperature of injected coal particles rises rapidly and when it reaches 100°C the *drying stage* begins. It is characterized by water evaporation from surface and micropores of solid fuel particles. At temperatures close to 300°C water is completely released from the fuel. Processes of heating and drying in fluidized bed take about 3–5 s for coal particle 3 mm in diameter.

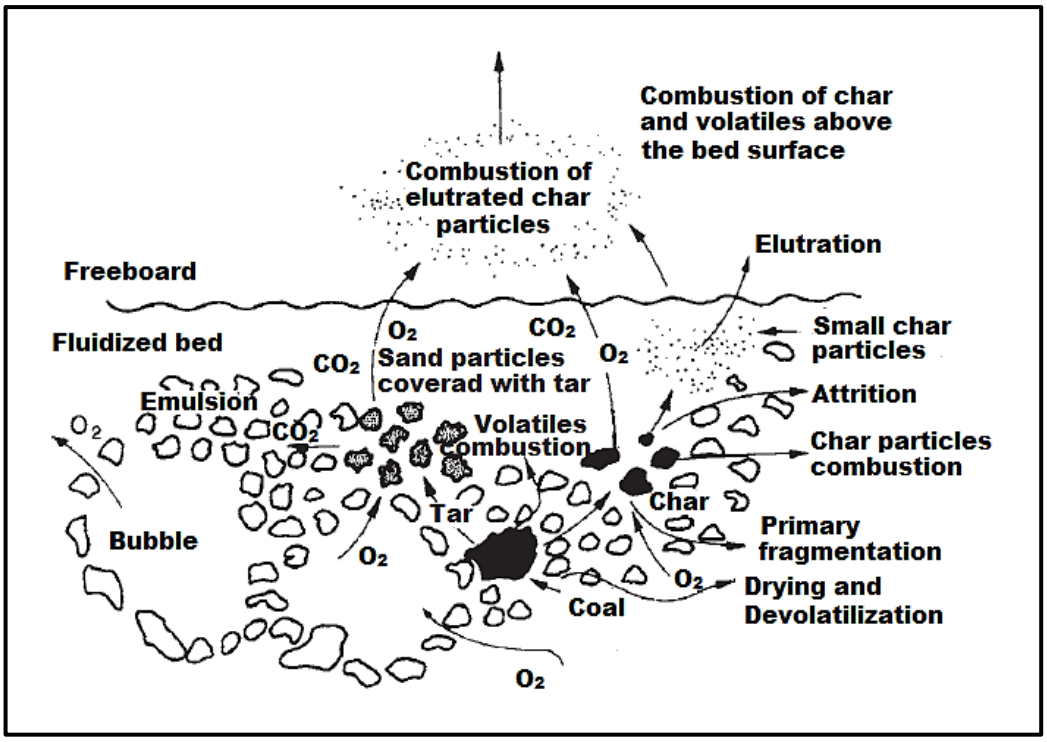

Fig. 4. Coal particle burning in the fluidized bed: scheme of the different processes **[3]**.

Further increase of temperature leads to decomposition of fuel organic constituents and formation of gaseous products. This stage is called *pyrolysis or devolatilization*. The process starts at temperatures above 300°C and has several stages. At the beginning tars and then gaseous products such as carbon dioxide (CO_2), methane (CH_4) and other light hydrocarbons (C_2H_6, C_2H_4, C_2H_2) are formed. Hydrogen (H_2), sulphur (S) and nitrogen (N) are released at the final stage of the process. Moisture and gaseous products rapid release may cause *fragmentation* of coal particle into several small particles. It occurs when pores of

the coal particle are too small to conduct all the volatiles and particle swell and then burst because of growing inner pressure.

Volatiles release looks like an upward cloud around the coal particle. This cloud diffuses the particulate (emulsion) phase (fig. 4) and ignites. *Ignition* occurs when volatiles release rate (depends on temperature) is enough for sustainable combustion and when sufficient amount of oxygen is present. Volatiles ignition temperature lies between 650 and 750°C. It depends on the fuel characteristics (volatile matter, ash and moisture content, fuel structure) and combustion conditions inside furnace. Ignition temperature is lower for fuels with high volatile content and for fine fuels.

Ignition leads to acceleration of oxidation process and considerable rise of temperature. When release rate is too high, a large amount of volatiles can't be burned near the particle. Unburnt volatile matter goes through the bed. A portion of it mixes with oxygen, ignites and burns in the fluidized bed volume. Another portion of volatiles leaves the bed and burns in freeboard zone. So it is very important to ensure secondary or even tertiary air supply for complete combustion of released volatiles above the bed.

Process of devolatilization in fluidized beds usually takes from 10 s to 100 s depending on the fuel type and particles size **[3]**. It occurs in a wide temperature range, from 300°C to 800°C.

Devolatilization and volatile combustion processes precede and often overlap the *combustion of char*. Char is formed when tars and gaseous products are released from solid fuel. The ignition temperature of residual char is much lower than volatiles ignition temperature and can be under 300°C (for lignite). In spite of this, char starts to burn only after release of volatiles, which envelope the particle and prevent its contact with oxygen. Simultaneous ignition of volatile matter and char is possible at high heating rates inside the furnace.

Char combustion occurs at the particle surface and inside pores and passes much slower than volatile combustion due to difficulties with oxygen diffusion through

emulsion phase to the fuel particles and its penetration to the pores. When oxygen reaches external particle surface, the reaction of carbon oxidation starts with subsequent formation of carbon monoxide (CO) and dioxide (CO_2). Under proper conditions oxygen gets into numerous pores and reacts with carbon on the pore walls.

Residual char combustion in fluidized bed takes much longer time than process of devolatilization and volatiles combustion (usually from 100 to 2000 s depending on particle size).

Combustion of char particles is accompanied by the process of *attrition*. Attrition occurs due to frequent collisions of fuel particles with each other and with inert material particles when little particles of char separate from the main particles. If the size of these particles is too small, they removed from the fluidized bed by air and combustion products flux. Usually elutriated particles have not enough time to be burnt in the freeboard zone. This causes combustion losses with unburnt carbon in fly ash.

4. BUBBLING FLUIDIZED BED BOILER: MECHANISMS OF FLUIDIZATION AND HEAT TRANSFER.

The basic difference between boiler types is in hydrodynamics of gas–solid motion inside the furnace. It defines the design of boiler and its operating characteristics. Changes in hydrodynamic regime influence significantly on boiler functioning. So, the comprehension of gas-solid motion mechanisms plays a significant role.

Another essential mechanism is heat transfer within the furnace space. Thermal efficiency of a boiler strongly depends on furnace design and heat transfer surfaces type and location. The detailed investigation of different heat transfer modes in BFB boiler allows to get temperature distribution along the boiler furnace and analyze the influence of various factors on it hereinafter.

4.1. Fluidization fundamentals.

Fluidization is a process at which granular material starts to behave itself as a fluid. It occurs when liquid or gas passes through granular material at a certain velocity.

As mentioned previously, this principle is used in fluidized bed boilers for efficient fuel combustion. Granular material which forms fluidized bed, in most cases consists of sand, solid fuel particles and specific additives (such as limestone). The hydrodynamics of fluidized bed, motion of particles in a freeboard zone, mechanism of heat transfer inside furnace space, process of fuel combustion considerably depend on physical properties of solid particles. Therefore physical properties of fluidized bed materials are reviewed in this section in detail.

4.1.1. Basic properties of particulate solids.

Fluidized bed material is a mechanical mixture of numerous solid particles. They have various shapes and different sizes as a result of natural processes (sand) or technological operations (fuel grinding). Physical characteristics of fluidized bed material are incorporated into numerous equations for calculation of different processes inside BFB boilers.

One of the main characteristics of fluidized bed material is bulk density, which equal to the mass of particles divided into bed volume:

$$\rho_b = \frac{m_b}{V_b} = \rho_p \cdot (1 - \varepsilon). \qquad (4.1)$$

Bulk density is smaller than the density of solid particles due to the volume of voids between particles included in the bulk volume V_b. Bulk density depends on density of solid particles, their size, shape and roughness of surface. Particulate materials are commonly classified according to their bulk density: from light (ρ_b < 600 kg/m^3) to heavy (ρ_b > 2000 kg/m^3). Materials formed fluidized bed (sand, limestone, solid fuel and ash) belong to medium materials (their bulk densitie are given in tab. 4).

Tab. 4. Bulk density of some particulate solids **[3]**.

Material	**ρ_b, kg/m^3**
Sand	1200–1400
Limestone	1200–1400
Coal	600–800
Ash	1200–1500

The porosity or void fraction of the bed is a ratio of volume of voids between particles and total volume of the bed:

$$\varepsilon = \frac{V_b - \sum V_p}{V_b} = 1 - \frac{\rho_b}{\rho_p}\,. \qquad (4.2)$$

Void fraction value can change from 0 to 100%. The higher the volume of voids, the higher the value of void fraction. Particulate solids used in fluidized bed boilers have void fraction value around 0.4–0.45 (for fixed beds) **[3]**. Change of void fraction value indicates change of fluidization regime.

Particles of bed material can have various shapes from regular sphere to sharp crystal. Uniform spherical particles have easy recognizable sphere diameter. Geometrical size of irregulary shaped particles is hardly defined. Meanwhile, it is needed for different calculations concerning fluidization regimes. For particles with irregular shape often a mean equivalent diameter is defined. There are different ways for mean equivalent diameter definition (mean arifmethical, geometrical, mean surface diameter and so on), each is used in calculation of certain process.

But the assumption that irregularly shaped particle can be considered as sphere of mean equivalent diameter is not always acceptable. Hydrodynamic properties of these particle are different from properties of regularly shaped (spherical) particle. For calculation of processes where particle external surface plays an important role, such shape factor as sphericity is used. It shows a conformity rate of irregular particle to ideal sphere:

$$\phi_s = \frac{A_s}{A_p} = \frac{V_p^{2/3}}{0.205 A_p}\,, \qquad (4.3)$$

where A_s and A_p are surface areas of sphere and irregular particle with the same volumes. For example, mean sphericity of sand is about 0.75, for stone coal 6 mm in diameter it is 0.54.

As to the classification of particulate materials by the particle size, one of the most commonly used divides particulate materials into lumps (d_{max}>10 mm), coarse

grained (d_{max}=2–10 mm), fine grained (d_{max}=0.5–2 mm), powder (d_{max}=0.05–0.5 mm) and pulverulent (d_{max}<0.05 mm).

4.1.2. Hydrodynamic properties of solid particles.

Fluidization is a process of interaction of numerous particles and fluid. Particles in fluidized bed move randomly, come into collision with other particles, often form short-lived clusters. For understanding and subsequent investigation of fluidization mechanism it is important to know hydrodynamic properties of a single particle taking part in the process.

One of the main concepts in particle hydrodynamics is a *terminal (or free fall) velocity*. It is an important characteristic value used in description of fluidized state. Free fall velocity of a particle and minimum fluidization velocity have the same physical essence **[3]**. It based on a balance of forces acting on a particle in fluidized bed. Value of free fall velocity determines upper bound of the fluid velocity at which it is possible to keep bed at a fluidized state. When the velocity of fluid passing through the fluidized bed reaches the terminal velocity of a single particle, further increase of fluid velocity will lead to carryover of the particle from the bed. Determination of free fall velocity plays an important role in calculation of various fluidization regimes and in analysis of energy losses with elutriated unburnt particles.

A spherical particle within the gravity field during its free fall in a static fluid is under the following forces:

– buoyancy (Archimedes) force

$$F_A = \rho_f g V_p \,, \tag{4.4}$$

– gravity force

$$F_G = \rho_p g V_p \,, \tag{4.5}$$

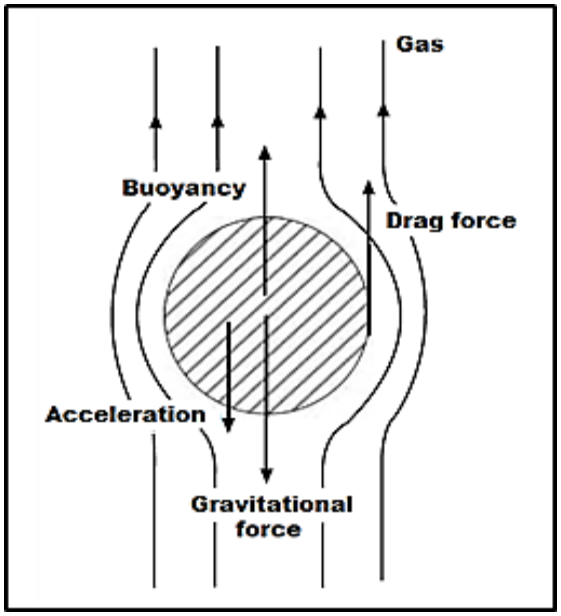

Fig. 5. Force balance of a particle moving in an upward gas stream **[2]**.

– drag force

$$F_D = C_d \frac{\pi d_p^2}{4} \cdot \frac{U_p}{2} \rho_f \, . \tag{4.6}$$

When a particle falls freely it uniformly accelerates under gravitational force. The buoyancy force and the drag force (also called hydrodynamic resistance) are opposite the gravity (fig. 5). Gravitational and buoyancy forces are constant and do not depend on the particle velocity, while drag force rises with the particle velocity until the balance of forces is achieved:

$$F_G = F_A + F_D \, , \tag{4.7}$$

$$m_p g = \rho_f g V_p + C_d \frac{\pi {d_p}^2}{4} \cdot \frac{\rho_f {U_f}^2}{2} \, . \tag{4.8}$$

After this, the particle continues to fall with a uniform (free fall) velocity only because of inertia, since the resultant force affecting the particle equal to zero. The same result is achieved in fluidized bed when the air flow reaches the value of free

fall velocity and the particle starts “to float” in the upward flow of air. There is also a balance of all forces acting the particle.

Equation (4.7) can be transformed to the dimensionless form:

$$Ar = \frac{3}{4} C_D {Re_t}^2. \qquad (4.9)$$

The left side of the equation (4.9) depends only on particle and fluid properties, while the right side contains drag coefficient C_D which is a function of Reynolds number. It depends strongly on velocity (flow regime) and particle shape and can not be expressed by a universal formula. Different approaches are used for determination of drag coefficient: tables, nomograms, various equations for certain diapasons of Re number proposed by differen authors.

For example, drag force coefficient can be found from the following relation **[2]**:

$$C_D = \frac{a_1}{Re^{\,b_1}}, \qquad (4.10)$$

where a_1 and b_1 are coefficients dependent on flow regime (Reynolds number). Approximated values are represented in the tab. 5.

Tab. 5. Constants for calculation of drag force coefficient C_D **[2]**.

Range of Reynolds number	**a_1**	**b_1**
0 < Re < 0.4	24	1.0
0.4 < Re < 500	10	0.5
500 < Re	0.43	0.0

4.1.3. Gas–solid fluidization regimes.

Fluidization technology is widely used in different industrial processes. It applied successfully for efficient fuel combustion. But the technology has a lot of specific

features concerned with the regime of fluidization. These features influence boiler design greatly and will be examined in this work in detail.

As follows from the above, fluidizes bed is formed by gas flow through a granular material resting on the bottom of the furnace. Increase in gas flow velocity leads to a number of changes in the moution of particles. Depending on the gas velocity, following states of the bed are defined: fixed bed, bubbling bed, turbulent bed, fast fluidization and pneumatic transport (fig. 6). The first and the last states are not referred to the concept of fluidization, but they are also reviewed as boundary regimes of the process.

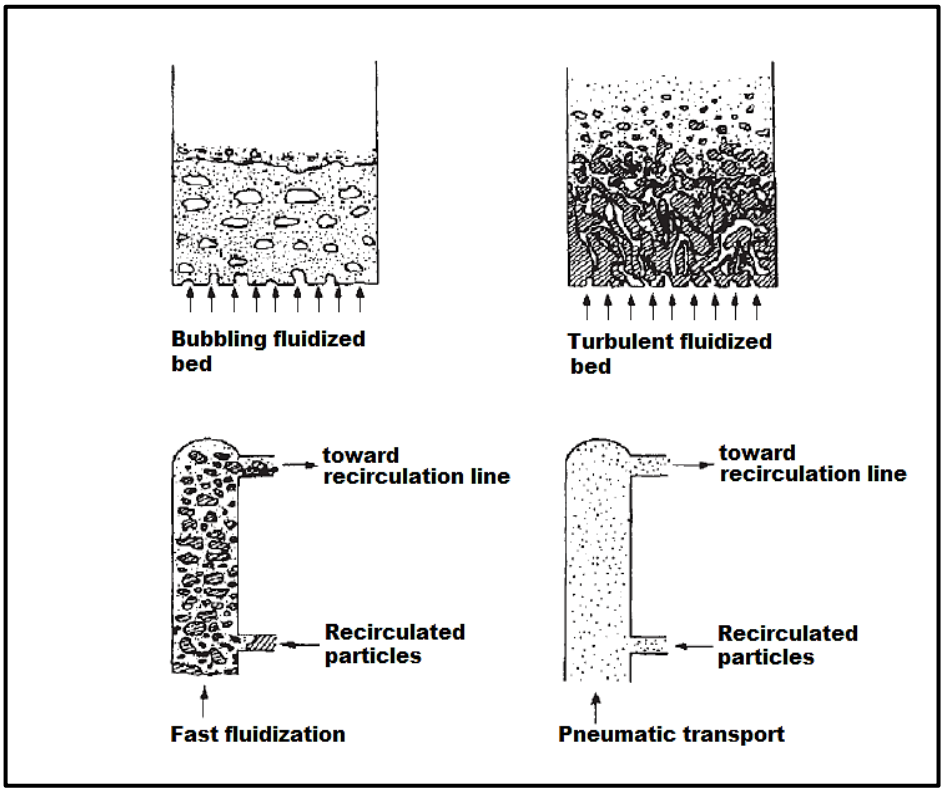

Fig. 6. Different fluidization regimes **[3]**.

A *fixed bed* can be considered as an initial state of the bed. In this state, gas supplied from the perforated bottom of vessel, flows through numerous voids between stationary particles. With increasing of gas velocity, resistance of bed material rises, but its height and surface shape still remains undisturbed. The

pressure drop during gas passing through the bed material in dependence on gas flow velocity and fluidization regime is shown in fig. 7.

When gas flow velocity reaches a critical value called *minimum fluidization velocity*, bed particles separate from each other and start to move. Height of the bed rises. At this moment pressure drop reaches its maximum and becomes equal to the weight of bed material per unit of cross-sectional area. Further increase of the fluidization velocity doesn't lead to significant changes of pressure drop value throughout the regime. Slight reduction of pressure drop on the graph (fig. 7) can be explained by elutriation of fine particles from bed surface, which causes bed weight decrease and thereafter decrease of resistance to gas flow.

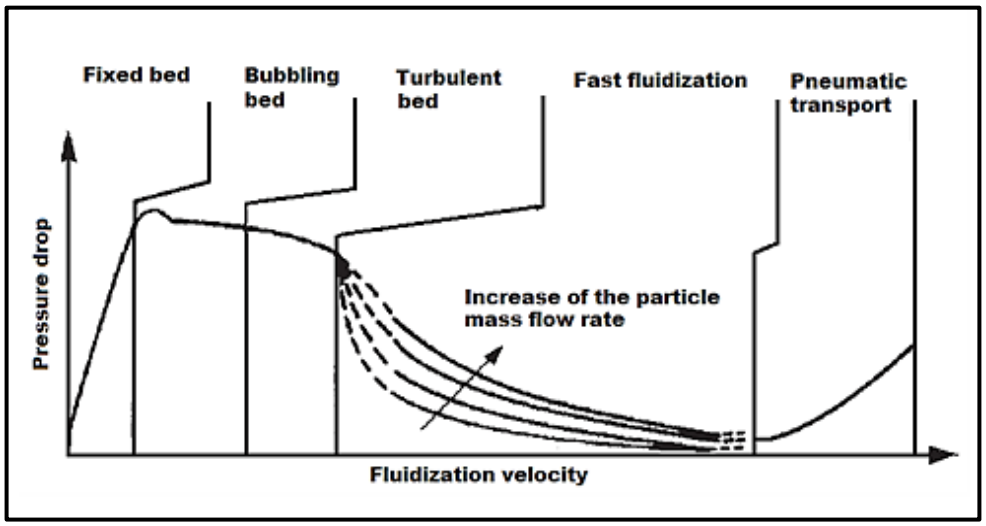

Fig. 7. Pressure drop in dependence of fluidization velocity for different fluidization regimes **[3]**.

Fluidized bed "bubbles" at gas velocities a few higher than minimum fluidization velocity (for most materials). From this moment, gas bubbles start to appear in the particulate (emulsion) phase of the bed. It leads to further expansion of the bed. Bubbles are formed in the bottom zone, rise through the bed and merge into large bubbles. When bubbles achieve bed surface, they burst and eject all the particles from their upper surface to the freeboard. Bubbles motion produces intense and organized circulation of particles inside the bed and their mixing with gas.

It is to be noted that there is a difference between bubbles motion in the bed formed by fine or coarse particles. Inside a fine bed material, gas in bubbles moves faster than gas in the particulate phase and they don't mix with each other. In the case of fuel combustion in fluidized bed, air in bubbles doesn't take part in the process of firing. Inside a coarse bed material, gas velocity in the particulate phase is higher than in bubbles, so mixing is possible.

In the range between the minimum fluidization velocity and the transport velocity, apart from bubbling fluidized regime, *turbulent fluidized regime* exists. The transition from bubbling to turbulent regime with increasing gas velocity is defined by formation of elongated, irregular-shaped voids instead of bubbles (fig. 6). Solid particle and gas mixing becomes more intensive. Regime change occurs in a wide range of velocities and characterized by pressure fluctuations.

Particles elutriation from the bed surface takes place during the all regimes of fluidization. With the beginning of turbulent fluidization regime, elutriation increases, but free surface of the bed is still defined. If elutriated particles return back, the bed height doesn't change. The concentration of elutriated particles decreases along the freeboard height till a certain value.

Developed turbulent fluidization regime is accompanied by formation of short–lived clusters of particles above the bed surface. Large clusters return into the bed, while small clusters may be carried away by gas flow. When gas velocity reaches the free fall velocity of the clusters, particle elutriation starts to rise and bed density significantly decreases (fig. 7). It means that *transport velocity* has been achieved and turbulent regime has changed to fast fluidization. With further velocity increase all particulate material will be removed from the bed (if there is no recirculating system).

Fast fluidization regime is characterized by moving of solid particles in clusters, most of which leave the freeboard space. There is no more definite bed surface. Particle mixing is much more intensive than in two previous regimes. Particles form clusters during their chaotic motion. If the clusters are too large to be carried away, they disintegrate and new clusters are formed.

Size of clusters depends on fluidization velocity and recirculation rate. Pressure drop and concentration of solids during fast fluidization also depend on recirculation rate. Thus, with increase of recirculation rate pressure drop also increases due to increase of bed density (fig. 7). With increase of fluidization velocity and decrease of recirculation rate, clusters become smaller and number of independent particles rises.

Further increase of velocity leads to transition from fast fluidization to *pneumatic regime*: particles start to move individually in a straight–line trajectory. Backward particle motion is absent. Transition occurs at a void fraction about 95%.

4.2. Bubbling fluidized bed hydrodynamics.

As the work focuses mainly on examination of processes inside BFB boiler furnace, it is required to pay more attention to hydrodynamics of bubbling fluidized bed.

4.2.1. Some features of bed mechanics.

Before beginning of fluidization particulate material lies static on the grate. Gas flows through irregular channels in the bed material and tries to overcome bed resistance. In the initial stage, when gas velocity is low, the regime is laminar and the resistance increases linearly. At the further increase of velocity, gas flow regime changes to turbulent and resistance becomes quadratic function of gas velocity. As it was mentioned above, fluidization takes place at velocities when flow resistance is equal to the particles' weight. Then distance between particles increases and bed expands. The small peak on the graph (fig. 7) at the initial stage of fluidization can be explained by overcoming of adhesive forces between particles.

Fluidization of most materials entails bubbles formation in the bed volume. But the moment when bed starts "bubble" and mechanics of the process depend

strongly on a type of bed material. Classification suggested by D. Geldart based on density and size of particles (fig. 8). It divides particulate material into four groups. *Group A* includes materials consist on particles of small size and low density (less than 1400 kg/m^3). Fluidization of such materials is achieved before the moment when bed starts to bubble. In bubbling fluidized bed gas velocity in particulate phase is lower than in bubbles. *Group B* is formed by materials of medium particle size and density. Most of inert bed materials (river sand, olivine) belong to this category. Bubbles occur in the bed of such materials right in the moment when minimum fluidization velocity is achieved. Gas in bubbles has velocity higher than in the particulate phase. Materials of *C group* are fine

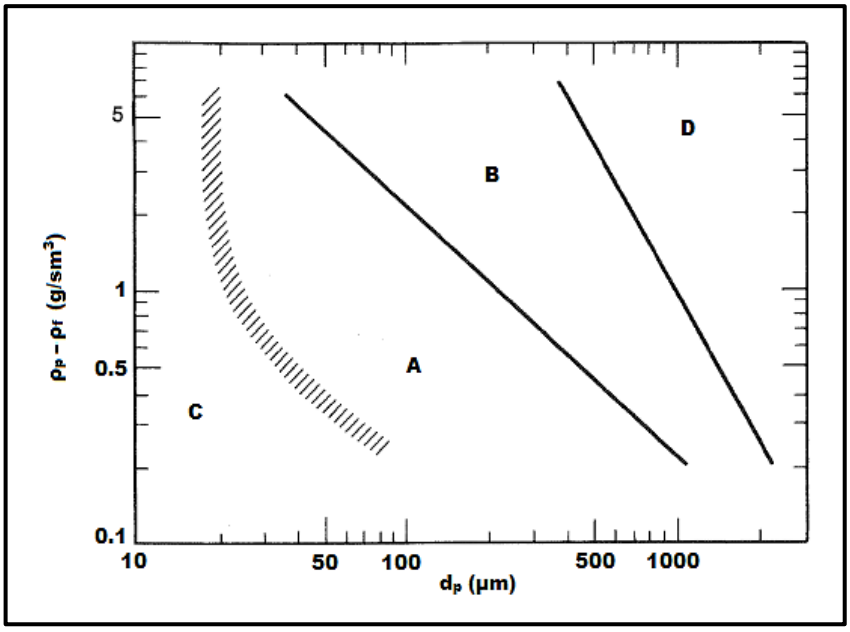

Fig. 8. Geldart's particle classification diagram **[3]**.

powders with predisposition to formation of channels hindering fluidization. *Group D* consists on materials from high-density coarse particles. During the fluidization of such materials air velocity in particulate phase is much higher than velocity of rising bubbles. Bubbling fluidized bed boilers use mainly materials of the group B (closer to the boundary with D group).

4.2.2. Minimum fluidization velocity.

Minimum fluidization velocity is the basic concept of fluidization studies. It has been defined for many particulate materials for the whole research history. As results of numerous experiments, there are a lot of correlations for determination of minimum fluidization velocity. Wen and Yu proposed a universal function, based on correlations for pressure drops in fixed and fluidized beds.

Gas flow through the fixed bed can be approximated to the flow through the branchy system of tubes with irregular shape and variable diameter. In that case, pressure losses in the bed can be described with common Darcy formula for a fluid flow through a round pipe:

$$\Delta p = \lambda \frac{L}{D} \cdot \frac{U^2}{2} \rho_f \,. \tag{4.11}$$

The next relation based on this formula, was proposed by Kozeny to calculate the pressure drop of a fluid flowing through a fixed bed of solids **[3]**:

$$\Delta p_b = H_b \frac{180(1-\varepsilon)^2}{\varepsilon^3} \cdot \frac{\mu_f U_f}{\left(\phi_s d_p\right)^2} \,. \tag{4.12}$$

For its transformation the following relations were used:

– total volume of voids in the bed material

$$V_\varepsilon = V_b - \Sigma V_p = \varepsilon V_b \,, \tag{4.13}$$

– mean hydraulic diameter for the fluid flow through the bed

$$D_h = \frac{6V_\varepsilon}{\Sigma A_p} = \frac{\varepsilon d_b}{\phi_s(1-\varepsilon)} \,, \tag{4.14}$$

– total surface of particles composing the bed

$$\Sigma A_p = \Sigma \pi \phi_s {d_p}^2. \tag{4.15}$$

Coefficient in the Kozeny–Carman equation (4.12) was received from experimental data for laminar flow through materials of A group. Modification of Kozeny–Carman equation proposed by Ergun is more universal and provides satisfactory results for a wide range of materials and flow regimes:

$$\Delta p_b = H_b \frac{150(1-\varepsilon)^2}{\varepsilon^3} \cdot \frac{\mu_f U_f}{\left(\phi_s d_p\right)^2} + H_b \frac{1.75(1-\varepsilon)}{\varepsilon^3} \cdot \frac{\rho_f {U_f}^2}{\phi_s d_p} . \qquad (4.16)$$

Mean particle diameter in the Ergun equation is determined as a ratio:

$$d_p = \frac{\sum_{i=1}^{n} n_i {d_{pi}}^3}{\sum_{i=1}^{n} n_i {d_{pi}}^2} . \qquad (4.17)$$

Pressure losses in the fluidized bed are equal to bed weight diminished by buoyancy forces:

$$\Delta p_b = (1-\varepsilon)\left(\rho_p - \rho_f\right) g H_b . \qquad (4.18)$$

The minimum fluidization velocity may be obtained by solving the equations (4.16) and (4.18) simultaneously taking into account that for different particulate materials the next approximation can be used:

$$\frac{1}{\phi_s {\varepsilon_{mf}}^3} \approx 14 \text{ and } \frac{1-\varepsilon_{mf}}{{\phi_s}^2 {\varepsilon_{mf}}^3} \approx 11 . \qquad (4.19)$$

After some rearrangements:

$$Re_{mf} = \frac{d_p U_{mf}}{\nu_f} = \left({C_1}^2 + C_2 Ar\right)^{0.5} - C_1 , \qquad (4.20)$$

where Archimedes number

$$Ar = \frac{\rho_f\left(\rho_p - \rho_f\right) g {d_p}^3}{{\mu_f}^2} . \qquad (4.21)$$

Constant values C_1 and C_2 are determined from experimental data: C_1=28.7, C_2=0.0494 for $d_p \geq 100$ μm and C_1=33.7, C_2=0.0408 for $d_p \leq 100$ μm **[16]**.

4.2.3. Maximum fluidization velocity (transport velocity).

Quite important moment in this work is to define boundaries of the bubbling fluidization. Thus, lower boundary of the process is minimum fluidization velocity at which fluidization starts. Upper bound is the transition from turbulent bed regime to fast fluidization. It can be approximated by free fall velocity of the smallest particle. There are a lot of correlations for transport velocity determination. Some of them are based on a ratio between minimum fluidization velocity and free fall velocity as values with the same nature (characterized by balance of forces acting on a particle in the upward gas flow). They all have quite high inaccuracy rate (about 30%) due to experiments with beds of small diameter. One of the most universal equations given by Perales **[2]** for diapason 20 < Ar < 50000 is:

$$U_t = 1.45 \frac{\mu_f}{\rho_f d_p} Ar^{0.484} . \qquad (4.22)$$

It was obtained from experiments that for bubbling fluidized beds of coarse particles the diapason of boundary velocities is quite narrow (about $10U_{mf}$) **[3]**, so it should be taken into account during determination of operational conditions.

4.2.4. Zoning of furnace and particle concentration.

With the beginning of fluidization process, bed formed by coarse particles (groups B and D) starts to bubble. Horizontal and flat, bed surface turns to irregular due to intensive bubbles bursting and solids ejection. Continuous fluctuations of the bed surface cause a big problem with accuracy of bed height determination. Meanwhile, it is an important parameter for the furnace designing. It has an influence on the refractory height and heat transfer surfaces location.

Bed height depends on gas flow velocity: with increase of velocity bed expands. Increase of bed height occurs due to change of bed material density:

$$\frac{H}{H_{mf}} = \frac{\rho_{mf}}{\rho_b} = \frac{1-\varepsilon_{mf}}{1-\varepsilon}\,. \tag{4.23}$$

There are a lot of correlations for determination of bed height in dependence of gas flow velocity **[3]**. They all are based on experiments and have low accuracy in a wide range due to large number of influencing parameters. Expansion of a bed formed from coarse particles (B or D group) can be determined by Davidson and Harrison ratio **[2]**:

$$\frac{H-H_{mf}}{H_{mf}} = \frac{U_f - U_{mf}}{U_{bm}}\,, \tag{4.24}$$

where U_{bm} – minimum bubbling velocity – can be equal to minimum fluidization velocity for coarse solids due to the fact that bed formed by coarse material starts bubbling right after achieving minimum fluidization velocity.

More accurate formula utilized for correlation of velocity and both bed height and porosity offered by Zaki and Richardson:

$$\frac{U_f}{U_t} = \varepsilon^n, \tag{4.25}$$

where power n depends on bed material type and can be defined the following way:

$$n = \frac{-log\frac{Re_t}{Re_{mf}}}{log\varepsilon_{mf}}. \tag{4.26}$$

Voidage at minimum fluidization velocity can be found using transformed equation (4.16):

$$Ar = \frac{1.75}{{\varepsilon_{mf}}^3\phi}{Re_{mf}}^2 + \frac{150(1-\varepsilon_{mf})}{{\varepsilon_{mf}}^3\phi^2}Re_{mf}. \tag{4.27}$$

Besides bed height and voidage, another important design parameter for bubbling fluidized bed boiler is a height of freeboard (space above bed surface). Concerning boilers with water wall tubes, freeboard height is generally defined by heat transfer surface area needed for evaporation. For reduction losses with unburnt fuel particles, freeboard height should exceed transport disengaging height (TDH).

Transport disengaging height relates to the concept of particle elutriation. Particles can be elutriated from the bed surface if gas flow velocity exceeds particle free fall velocity. Also elutriation of particles from fluidized bed surface is caused by intensive bursting of bubbles and ejection of particles (often in clusters) with high velocities into freeboard. Injected clusters move upward, disintegrate to the small clusters and single particles. Particles with terminal velocities lower than gas flow velocity are carried over, while others return back to the fluidized bed. Near furnace walls, the amount of falling particles is higher due to lower gas velocities. As the distance from bed increases, the amount of rising particles and falling clusters also increases. At a certain height, there are only rising particles (dilute zone).

Difficult process of solids motion in the freeboard space leads to considerable changes in particle concentration (or emulsion density) along the furnace height: it decreases with the height until constant value is achieved. It can be assumed that over the bed volume emulsion density remains steady, whereas in the splash zone where bubbles burst and erupt solids, it changes gradually. Erupted particles move upward due to the impulse and drug force. From the moment gas drag doesn’t exceed particle weight, particle disengages from the flow and gravity force returns it to the fluidized bed. Along the height of freeboard, amount of such particles decreases by the exponential law till a certain height where it is equal to zero. This height is known as transport disengagement height. Only particles with weight less than gas drag overcome this height and leave the furnace. In other words, it is possible for particles with terminal velocities lower than gas flow velocity.

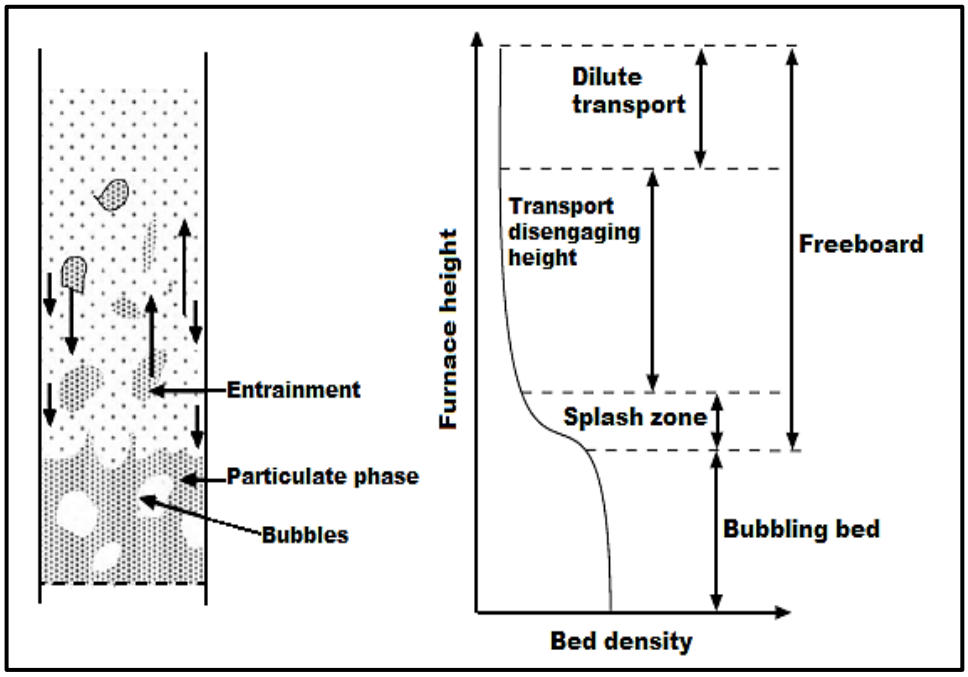

Fig. 9. Bubbling fluidized bed: particle motion and mean particle density along the furnace height **[2]**.

There are a lot of empirical correlations for determination of TDH, but most of them are derived from experiments with fine particles and beds of a small diameter, so they have high accuracy usually in a narrow range. For calculation of TDH for boiler furnaces the equation of Chan and Knowlton **[27]** can be used:

$$TDH = 0.85{U_f}^{1.2}(7.33 - 1.2logU_f)\,, \tag{4.28}$$

Density in the freeboard space complies with the Gaussian probability distribution:

$$\rho = \rho_\infty + (\rho_0 - \rho_\infty)e^{-a_f(h-H_b)}, \tag{4.29}$$

where a_f is a constant showing the change of entrainment flux of solids with the distance from the bed surface. It is determined from empirical correlations and ranges from 3.5 to 6.4 m^{-1}. In **[17], [24]** it is recommended to use a_f = 4 m^{-1}. Typical values for density above the transport disengaging height ρ_∞ is around 10^{-3}–10^{-4} kg/m^3 for most BFB boilers.

4.3. Heat transfer.

There are some specific features which differ fluidized bed boilers from conventional boilers. In comparison to conventional boilers, fluidized bed boilers have lower combustion temperatures (about 900°C) and higher concentration of solids in the furnace space. The last feature specifies heat transfer mechanisms inside furnace: besides gas convection and radiation, heat transfer by contact of particles takes place. All posible mechanisms of heat transfer in the furnace of bubbling fluidised bed boiler and equations for estimation of heat transfer coefficients are reviewed in this section.

4.3.1. General aspects.

Average furnace temperature of bubbling fluidized bed boiler doesn't change considerably along the height. Temperature inside the fluidized bed is uniform and amounts to 800–900°C. Intense heat exchange in the bed volume between hot particles and cold incoming air allows to maintain average bed temperature even near the distribution grate. It is to be noted that during combustion of fuels with high volatile content temperature in the freeboard can exceed bed temperature. Freeboard temperature changes both in longitudinal and transverse directions.

Particle concentration and its variation along the furnace height influence considerably heat exchange processes. Thus, in the fluidized bed concentration of solids may achieve 10^3 kg/m^3, while at the furnace outlet it is near 0.1 kg/m^3. Depending on concentration change, one or another heat transfer mechanism plays a more important role in the heat exchange process. In the immediate region of the fluidized bed, heat transfer by particles is predominant and radiation component of heat transfer often neglected **[3]**, while in the freeboard space radiation mechanism prevails. Hot bed material also irradiates to the furnace walls.

Intensity of heat transfer process is characterized by heat transfer coefficient. The typical ranges of heat transfer coefficients for different regions of a bubbling fluidized bed boiler are presented in the tab. 6.

Tab. 6. The typical range of heat transfer coefficients on different sections of a BFB boiler **[2]**.

Location	Type of Section	Typical heat transfer coefficients ($W/m^2 \cdot K$)
Water wall tubes above refractory in the furnace	Evaporator	150–190
Tubes placed across furnace	Superheater	180–220
Horizontal cross-tube heat exchanger in back–pass	Economizer, superheater, preheater	70–80
Gas-to-bed material	Furnace bed	30–200

In fluidized bed boilers considerable share of heat is transferred to the surface of water wall tubes. Sometimes immersed heat exchangers are used, but such cases are not considered in this work. Heat transfer intensity depends on many factors: gas flow character, size of particles and their concentration near the surface, surface geometry.

As to the heat transfer inside the fluidized bed, it is performed by interaction of gas and solid particles. Process of incoming air heating is very intensive due to large contact area (about 40000 m^2/m^3). There is almost no difference between air and particles temperatures inside the bed (except the aria near distribution grate). Local bed overheating may occur when fuels with high volatile matter are fired. In order to exclude such problem, it is required to learn process of diffusion in fluidized bed in detail. Fuels with high moisture and ash contents can be successfully burnt fluidized bed boilers due to rapid process of heating in the bed of hot particles. But the process of heat exchange between inert bed material and fuel particles should be studied thoroughly for efficient implementation of combustion.

4.3.2. Heat transfer process between gas and solids in a bubbling fluidized bed.

As it was mentioned above, temperature in the volume of fluidized bed is almost uniform (fluctuation is no more than 5°C). And gas flow outcoming from fluidized bed also has temperature of the bed. Heat transfer coefficient for hot particles to gas is quite low (about 20 $W/m^2 \cdot K$), so high ability of the fluidized bed to the heat exchange is explained by large contact surface between gas and solids. There are a lot of empirical correlations for heat transfer process calculation in fluidized beds, but the results can vary significantly due to difficulties related to experimental measurements and data processing.

Standard correlation for a single particle dropped into the bed of particles at average temperature was presented by Ranz and Marshall **[2]**:

$$Nu_p = 2 + 0.6{Re_p}^{0.5}Pr^{0.33}. \quad (4.30)$$

Later the equation for calculation of heat transfer coefficient for a whole bed was received (for 0.1<Re<200) **[3], [30]**:

$$Nu_b = \frac{\alpha_{gp} d_p}{\lambda_g} = 0.03{Re_p}^{1.3}. \quad (4.31)$$

As to the region near distribution grate, temperature difference between cold gas and hot particles vanishes after some millimeters from grate. The larger the size of solid particles, the larger the distance due to less contact area between particles and gas. In bubbling fluidized beds the temperature equalization is a complex process between particles and gas in bubbles and emulsion phase. In beds of coarse material gas circulation between bubbles and emulsion is intensive and temperature is equalized quickly. Particles which get into bubbles also promote the process of temperature equalization. For bubbles with small initial diameter gas temperature becomes equal to the particle temperature at the same distance as

for gas in the emulsion phase. This distance can be determined with the following equation:

$$L_{max} = \frac{U_o r_o T_b}{0.168 U_f Ga^{-0.1} T_o} . \quad (4.32)$$

4.3.3. Heat transfer between fuel particles and bubbling fluidized bed.

When particulate fuel injected to the fluidized bed it passes through stages of heating, drying and pyrolysis. It requires heat which is transferred from the fluidized bed to fuel particles. When ignition occurs and process of volatile and char combustion starts, fuel particle temperature rises and becomes higher than temperature of the bed. The direction of heat transfer changes.

Between particulate fuel and fluidized bed heat is transferred by gas convection, thermal conduction and radiation (may be neglected). One or another mechanism may prevail depending on the fuel particle size. When fuel particles are smaller than bed material particles heat convection dominates. Heat transfer by contact with other particles plays more important role for coarse fuel.

Experimental data shows influence of the most important parameters on fuel particle to bed heat transfer **[3]**. Thus, fluidization velocity affects heat transfer greatly. With the increase of bed material particle size, heat transfer decreases. Thermal conduction (heat transfer by particle contact) plays more significant role in heat transfer process than gas convection.

For fuel particles smaller than bed particles size, it is recommended to use for heat transfer calculation correlation (4.31). For fuel particles comparable to bed particles (group B) heat transfer may be calculated using value Nu=10. For beds formed by large particles the following correlation is recommended **[30]**:

$$Nu_p = 10 + 0.23(ArPr)^{1.3}. \quad (4.33)$$

Numerous formulae for heat transfer between fuel particles and fluidized bed show that this mechanism isn't investigated enough and required more experimental research. For estimation of heat transfer presented correlations can be used, but their accuracy is satisfactory only for calculation of process in conditions close to experimental.

4.3.4. Freeboard heat transfer.

In most cases, walls of fluidized bed boilers from refractory to furnace exit are covered with water tubes. Water wall tubes play an important role in the process of heat generation. For water wall tubes, the conditions of heat exchange vary greatly in dependence on furnace region. Lower part of tubes can be in contact with fluidized bed (rarely due to high erosive factor). In the freeboard space tubes are washed by hot gases and entrained particles, but the concentration of particles diminishes with the height and intensity of heat transfer decreases.

For calculating of heat transfer between water tubes and fluidized bed correlations for immersed heat transfer surfaces can be used, but this issue is beyond the scope of this work. Mainly this work is focused on calculating of heat transfer processes in the freeboard space of the BFB furnace. In the first approximation, formulae for pulverized boilers can be used. For more accurate calculations, there is methodology taking into account hydrodynamic of the process inside freeboard space and change of particle concentration both in longitudinal and transverse directions **[18]**. It is based on experiments on a large scale object (16 MW_{th} fluidized bed boiler) and obtained correlations can guarantee feasible accuracy in calculation of heat exchange processes inside industrial boilers. They show very good accordance to results of subsequent measurements.

As was mentioned previously, difference of heat transfer mechanisms in fluidized bed boilers is explained by change of particle concentration along the furnace space. Measurements in **[18]** confirm the dependence of heat transfer coefficient from particle concentration. The value changes from 650 $W/m^2 \cdot K$ in the fluidized

bed (for immersed surfaces and refractory lining) to 60 W/m^2 ·K near the furnace outlet. As evident from the fig. 10, heat flux to tube surface reaches a maximum value at the level of fixed bed height. It changed rapidly along the bed height and near the bed surface amounts to 50% of the maximum value. Splash zone is also characterized by high heat transfer coefficients to the walls due to intensive process of particles ejection.

In the freeboard zone far from fluidized bed heat flux to the tube surface reduces due to decrease of average concentration of hot particles in the volume and due to particle downward motion along the furnace walls. It is to be noted that near the walls particles concentration is almost two times higher than average and the size of particles also exceeds average value.

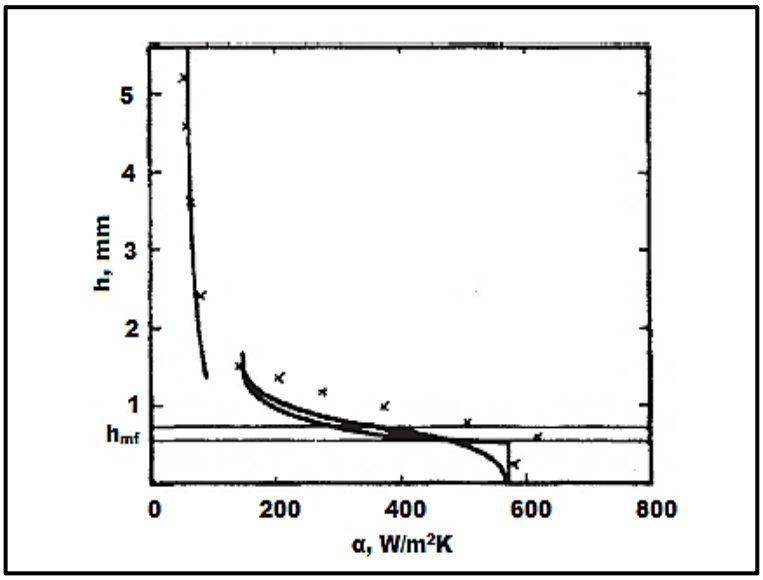

Fig. 10. Heat transfer coefficient along the furnace wall, from distribution plate to the furnace exit. Comparison of measured and calculated values **[18]**.

All the significant conditions were taken into account in the calculation methodology presented in **[18]**. The following correlations were proposed for calculating of heat transfer processes in the furnace of fluidized bed boiler.

Total heat transfer coefficient is represented as a sum of coefficients characterizing heat transfer by particles, gas flow and radiation:

$$\alpha = \alpha_{pc} + \alpha_{gc} + \alpha_{rad}\,. \tag{4.34}$$

Heat transfer by particle convection is calculated in the following manner:

$$\alpha_{pc} = \frac{\lambda_g}{d_p}(1-\varepsilon)Z(1-e^{-N}), \tag{4.35}$$

where

$$Z = \sqrt{\frac{g{d_p}^3(\varepsilon-\varepsilon_{mf})}{5(1-\varepsilon_{mf})(1-\varepsilon)}}\cdot\frac{1}{6}\cdot\frac{\rho_p c_p}{\lambda_g}\,, \tag{4.36}$$

$$N = \frac{Nu_{wp}}{C}\cdot Z\,, \tag{4.37}$$

$$\frac{1}{Nu_{wp}} = \frac{1}{(Nu_{wp})_{max}} + \frac{\lambda_g/\lambda_p}{4\left(1+\sqrt{\frac{3}{2}\cdot\frac{C}{\pi}\cdot\frac{\lambda_g}{\lambda_p}\cdot Z}\right)}\,, \tag{4.38}$$

$$(Nu_{wp})_{max} = 4\left[(1+Kn)\ln\left(1+\frac{1}{Kn}\right)-1\right], \tag{4.39}$$

$$Kn = \frac{4}{d_p}\left(\frac{2}{\gamma}-1\right)\frac{\lambda_g\sqrt{2\pi R T_b/M_g}}{p(2c_g - R/M_g)}\,, \tag{4.40}$$

$$\gamma = \left(1+10^{[K_1-(1000/T_p+K_2)]/K_3}\right)^{-1}, \tag{4.41}$$

where constant C varies in the range 1.0–4.0, other constants are K_1=0.6, K_2=1, K_3=2.8.

For calculation of the heat transfers process in the fluidized bed, it might be assumed that ρ_p=const (ε=const) to the level of the fixed bed, and in the splash zone:

$$\frac{\rho}{\rho_b} = \exp\left(-\frac{h-H_{mf}}{\bar{H}-H_{mf}}\right), \tag{4.42}$$

where $\overline{H}$ is bed height when the linear change of bed pressure turns to zero. The value of particle concentration above the splash zone (in the freeboard) is assumed to be constant and equal to particle concentration near the furnace outlet.

Radiative component of heat transfer coefficient is small at temperatures below 600°C. At typical operating temperatures of fluidized bed boilers (around 900°C) it has a considerable share in total heat transfer coefficient. Heat transfer by radiation according to Andersson model is calculated using the equation:

$$\alpha_{rad} = \frac{\sigma({T_b}^4 - {T_s}^4)}{\left(\frac{1}{\varepsilon_s} - \frac{1}{\varepsilon_{bs}} - 1\right) \cdot (T_b - T_s)}, \tag{4.43}$$

where, in the dense fluidized bed:

$$\varepsilon_{bs} = \left[\frac{\varepsilon_s}{(1-\varepsilon_s)B} \cdot \left(\frac{\varepsilon_s}{(1-\varepsilon_s)B} - 2\right)\right]^{0.5} - \frac{\varepsilon_s}{(1-\varepsilon_s)B}. \tag{4.44}$$

Constant B=0.667.

In the space with low particle concentration such as a freeboard:

$$\varepsilon_{bs} = \varepsilon_g + \varepsilon_m - \varepsilon_g \varepsilon_m, \tag{4.45}$$

where

$$\varepsilon_m = 1 - e^{-\sigma_p L_b}. \tag{4.46}$$

L is a mean beam length:

$$L_b = 3.5 \frac{V_F}{A_F}. \tag{4.47}$$

The radiation absorption coefficient of the particles can be found using the formula:

$$\sigma_p = \varepsilon_p n \frac{\pi {d_p}^2}{4}, \tag{4.48}$$

where

$$n = \frac{6\rho_m}{\rho_p \pi {d_p}^3}\,. \tag{4.49}$$

The process of heat transfer by gas convection in dense bed is described by the following correlation:

$$Nu_{gc} = 0.009 Pr^{1/3} Ar^{1/2}. \tag{4.50}$$

In the freeboard space:

$$\frac{\alpha_{gc} h}{\lambda_g} = 0.332 Pr^{1/3} {Re_h}^{1/2}. \tag{4.51}$$

Less cumbersome calculation of heat transfer coefficient in a freeboard zone of BFB boiler may be carried using the correlation of Andeen and Glicksman **[27]**, **[29]**:

$$\alpha = 900(1-\varepsilon)\frac{\lambda_f}{d_{to}}\left(\frac{U_f d_{to}\rho_f}{\mu_f}\cdot\frac{{\mu_f}^2}{{d_p}^3\rho_f\rho_p g}\right)^{0.326} Pr^{0.3} + \\ + \frac{\sigma({T_b}^4 - {T_s}^4)}{\left(\frac{1}{\varepsilon_s}+\frac{1}{\varepsilon_b}-1\right)\cdot(T_b - T_s)}. \tag{4.52}$$

It is represented as a sum of convective and radiative components of the total heat transfer coefficient. First term of the correlation implies both particle and gaseous convection the last of which is considerably heightened by presence of solid particles.

5. MODEL DEVELOPMENT.

The present part of the work is focused on creation of furnace model with use of programing methods (Simulink MATLAB), simulation of temperature regimes inside it and discussion of obtained results. It also includes preliminary stage of basic values determination and furnace design aspects.

5.1. Some basic aspects of furnace design.

Basic furnace design includes determination of dimensions (height, width and breadth), surface area of water wall tubes, height of bed and freeboard.

There is no unique algorithm for determination main design parameters. Thus, bed area of a furnace can be calculated by the following equation:

$$A_b = \frac{Q_c}{q_{cs}}, \tag{5.1}$$

where Q_c is combustion heat rate and q_{cs} is cross section heat load. Typical cross section heat loads for BFB boilers are in the range 1–3 W/m^2·K (higher for furnaces with in-bed tubes) **[2]**. Ratio of two cross section sides typically is about 1.02 **[21]**.

Bed height is generally between 0.5 and 1.5 m and depends on presence of in-bed tubes and type of fired fuel. Bed height can be determined using typical values of pressure drop over the bed 6–12 kPa.

Freeboard height is defined by necessary wall tubes area. Also it is recommended to choose freeboard height over transport disengaging height due to reduce combustion losses.

As to the furnace walls of a BFB boiler, they are formed by vertical tubes performing evaporative function in a water-steam cycle. Tubes can be welded to

each other or joined by fins welded between them. Fins increase heat transfer and form rigid gas-tight construction for the furnace. The mostly used material for wall tubes and fins is cheap and easy to shape low-carbon steel. The external surface of tube walls is typically covered with insulation (ceramic fiber in several layers) supported by studs and steel cladding.

The near-bottom furnace zone in addition has inner lining which protects lower parts of water tube walls both against high temperatures and intensive erosion as consequence of contact with hot abrasive particles. So, lining height typically exceeds the height of fluidized bed. The materials mainly used for furnace inner lining – bricks from chamotte or fire clay, high-alumina cement – have low coefficients of heat conductivity (0.8–1 W/m·K).

The thickness of the lining layer is defined according to specified heat losses:

$$Q_{bl} = A_l \frac{\Delta T_b}{R_l}, \tag{5.2}$$

where A_l is the total area of lining, ΔT_b is the temperature difference between bed and outside of the lining, R_l is the thermal resistance of lining. Final lining thickness should be corrected by erosion factor.

The same principle can be used to define thickness of insulating covering of boiler walls. External heat transfer coefficient for furnace walls in this case can be defined using Frank formula:

$$\alpha_e = 7.34{U_w}^{0.656} + 3.78e^{-1.91U_w}, \tag{5.3}$$

where U_w is wind velocity. First term of the formula (5.3) takes into account forced convection, while second defines natural convection. As evident, in the presence of wind second term approaches zero and heat transfer is performed mainly by forced convection.

As to geometry of wall tubes, typical value of tube diameter is in the range 30–80 mm and depends on specified pressure drop value. Required minimal thickness of water wall tubes can be found using the formula:

$$\delta_{wt} = \frac{d_{to} p}{\left(2\frac{\sigma_l}{n} - p\right) \cdot \nu + 2p} + C_1 + C_2, \quad (5.4)$$

where d_{to} is the outside tube diameter, p is the design pressure of the fluid, σ_l is the material strength, n is a safety factor (usually 1.5), ν is a strength factor (usually 1.0 **[22]**), C_1 is the additional thickness (about 10% of the tube wall thickness) and C_2 takes into account metal corrosion (depends on corrosion rate and boiler durability). It is to be noted that diameter and thickness of tube should comply with special technical standards (DIN, NPS, EN).

5.2. Water-steam circuit.

Mass balance of water and steam flows allows to define unknown components:

$$m_{ms} = m_{fw} + m_{ds} - m_{bd}, \quad (5.5)$$

where m_{ms} is main steam flow, m_{fw} is feed water rate, m_{ds} is amount of water for desuperheating and m_{bd} is blow down value. Typically, desuperheating water demand is about 9.5% from main steam flow and about 3% from main steam flow is blow down water rate.

When water and steam flows are defined it is possible to determine total heat demand as a basic characteristic for the process of steam generation and evaporative heat demand required for estimation of wall tubes heat transfer surface area and values of heat flows inside the furnace.

Expression for calculation of basic heat demands are represented below:

– economizer heat demand:

$$Q_{eco} = m_{fw}\left(h_{fwo}\left(t_{fwo}; p_{fwo}\right) - h_{fwi}(t_{fwi}; p_{fwi})\right), \quad (5.6)$$

where feed water outlet pressure p_{fwo} is typically 5% less inlet pressure due to losses in economizer. In order to prevent boiling of feed water in economizer tubes, the feed water outlet temperature t_{fwo} is usually 20-30°C lower than saturation temperature.

– superheater heat demand:

$$Q_{sh} = (m_{ms} - m_{ds})\left(h_{ssh}(t_{ssh}; p_{ssh}) - h_{ss}(p_s)\right) + \\ + m_{ds}\left(h_{ssh}(t_{ssh}; p_{ssh}) - h_{fwi}\left(t_{fwi}; p_{fwi}\right)\right), \quad (5.7)$$

where superheated steam pressure p_{ssh} is typically 10% less saturated steam pressure p_{ss} due to losses in superheater.

– total heat demand:

$$Q_{tot} = m_{ms} \cdot h_{ssh}(t_{ssh}; p_{ssh}) + m_{bd} \cdot h_{ws}(p_s) - \\ -\left(m_{fw} + m_{ds}\right) \cdot h_{fwi}\left(t_{fwi}; p_{fwi}\right). \quad (5.8)$$

– evaporative heat demand:

$$Q_{ev} = Q_{tot} - Q_{sh} - Q_{eco}. \quad (5.9)$$

– air preheating heat demand:

$$Q_{ap} = m_a \cdot c_{pa}\left(t_{ap} - t_a\right), \quad (5.10)$$

where t_a is the ambient temperature.

5.3. Bed heat balance.

As it was mentioned above, bed temperature is one of the main operating parameters for BFB boiler. It is controlled by air rate through the bed, fuel feed and also use of flue gas recirculation. Constant bed temperature maintenance

reduces upset conditions caused by fluctuation of fuel characteristics (moisture and ash content, heating value). Bed temperature should be higher the fuel ignition temperature and lower softening temperature in order to exclude formation of agglomerations in the bed. Typical bed temperatures of BFB boilers are in the range 800–850°C **[28]**. Heat balance of the bed allows to determine amount of primary air at which required bed temperature is maintained.

The process of fuel combustion in most cases isn't complete in the volume of fluidized bed. Usually volatiles and small fuel particles burn down in the freeboard space. The amount of heat released in the bed during partial fuel combustion can be found by following expression:

$$Q_b = m_f X_b HHV, \tag{5.11}$$

where m_f is the fuel feed and X_b is the bed combustion fraction.

Heat coming to the bed with primary air:

$$Q_{api} = m_{ap} X_b c_{pa} t_{api}\,, \tag{5.12}$$

where c_{pa} is the specific heat of air at constant pressure and t_{api} is the temperature of preheated air.

Heat brought to the bed with fuel and sorbents (limestone) also includes latent heat of solids moisture content:

$$Q_{fi} = (m_f c_{pf} + m_s c_{ps}) t_a + \left(m_f \omega_{wf} + m_s \omega_{ws}\right) h_a, \tag{5.13}$$

where c_p is solids specific heat and h_a is moisture enthalpy at ambient temperature; ω_{wf} and ω_{ws} are moisture fractions of solids.

These constituents form total heat input. Heat output is also a constitutive value. A main source of bed heat losses is heat radiated from bed surface:

$$Q_{br} = \sigma \varepsilon_b A_b \left({T_b}^4 - {T_{fb}}^4\right). \tag{5.14}$$

Heat losses with ash and sorbent removed from the bed are:

$$Q_d = \left(m_f \omega_a x_{da} c_{pash} + m_s x_{ds} c_{ps}\right) t_b, \quad (5.15)$$

where ω_a is ash content in the fuel and x_d is the share of the total ash and sorbent amount drained from the bed (about 40% from total ash amount for BFB boilers).

Fly ash and water vapor are carried over with flue gases. So, total heat loss with flue gases is:

$$Q_{fg} = m_{fg} c_{pfg} t_b + m_f \omega'_{wf} h_b + (1 - x_d)\left(\omega_a m_f c_{pash} + m_s c_{ps}\right) t_b, \quad (5.16)$$

where h_b is the enthalpy of steam at bed temperature and M_{fg} is amount of flue gases per 1 kg of burned fuel.

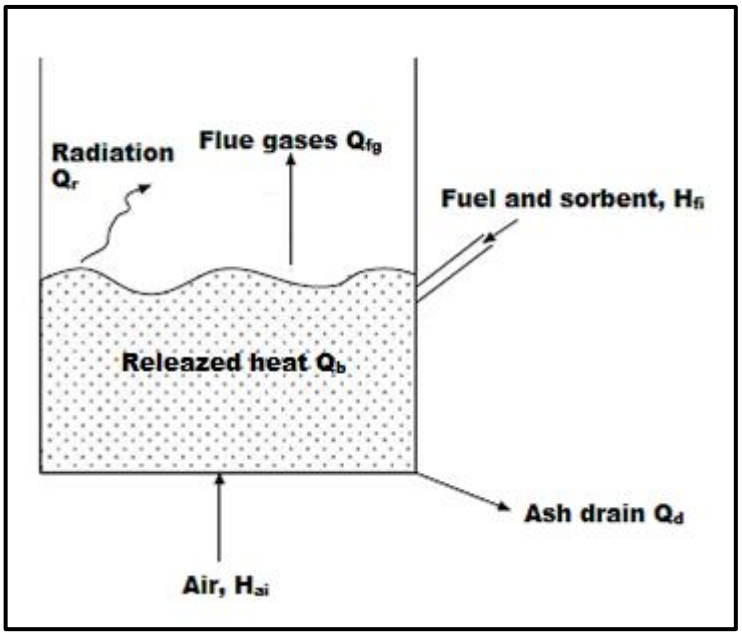

Fig. 11. Heat balance in a bubbling fluidized bed. **[2]**.

Heat balance is achieved when the total heat input is equal to the total heat output:

$$Q_b + Q_{api} + Q_{fi} = Q_{br} + Q_d + Q_{fg}. \quad (5.17)$$

It is required to solve the equation (5.17) for determination of primary air amount.

Mass balance of the furnace is represented below. Using the balance it is possible to define flue gases amount released during fuel combustion:

$$m_a + m_f = m_{fg} + \omega_a m_f, \tag{5.18}$$

where ω_a is fuel ash content.

5.4. Simulation object and initial data.

A real BFB boiler (fig. 12) with its operational characteristics represented in tab. 7 is taken as an object for modeling. It was built as a part of Kymin Voima, a biomass power plant in Kuusankoski, Finland. The power plant produces electricity and heat for Kymi paper mill and nearby towns Kuusankoski and Kouvola.

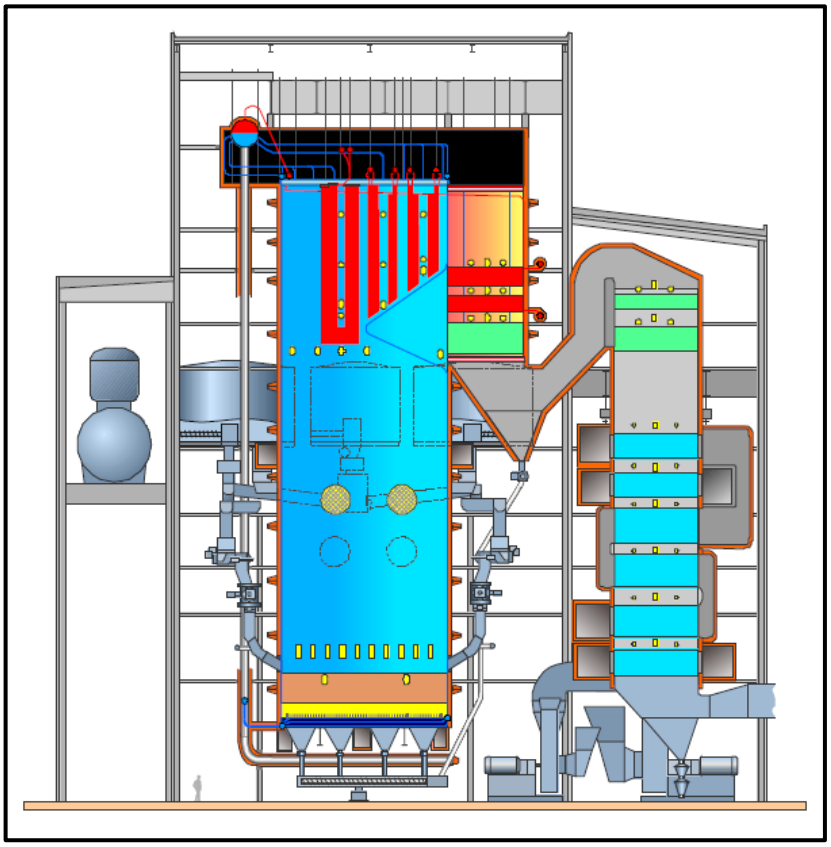

Fig. 12. BFB boiler, Kymin Voima, Kuusankoski. Source: Valmet Corporation.

Tab. 7. Operational characteristics of Kuusankoski BFB boiler.

Total power, MW	269
Overall efficiency, %	90.7
Steam amount, kg/s	107
Steam pressure, bar	114
Steam temperature, °C	541
Feed water temperature, °C	200
Combustion air temperature, °C	300

Such types of fuel as peat, wood biomass and wastes of pulp and paper mill can be successfully fired or co-fired in the present boiler. Characteristics of biomass (sawdust) as a possible fuel for boiler are indicated in tab. 8.

Tab. 8. Typical proximate and ultimate analyses for sawdust **[11]**.

Proximate analysis, %	
Fixed carbon	9.35
Volatile matter	55.03
Ash	0.69
Moisture	34.93
Ultimate analysis, %	
Carbon	32.06
Hydrogen	3.86
Oxygen	28.19
Nitrogen	0.26
Sulphur	0.01
Ash	0.69
Moisture	34.93

5.5. Determination of some characteristic values.

Fuel heating value – one of the most important fuel characteristics which shows the amount of heat released during combustion of 1 kg of fuel. The difference

between higher heating value (HHV) and lower heating value (LHV) is in the latent heat of water vapour contained in the combustion products:

$$HHV = LHV + r\frac{\omega_w + 9\omega_H}{100\%}, \tag{5.19}$$

where ω_w is the fuel moisture content and ω_H is the amount of hydrogen reacting with oxygen in the fuel and forming water. Numerical coefficient 9 shows that during the reaction of 1 kg of hydrogen with oxygen 9 kg of water is produced.

Percentage of hydrogen taking part in the reaction with fuel oxygen can be found from the proportion:

$$\begin{array}{ccccc} x & & \omega_{O2}\,\% & & y \\ 2H_2 & + & O_2 & \rightarrow & 2H_2O \\ 4\ \text{g/mole} & & 32\ \text{g/mole} & & 36\ \text{g/mole} \end{array}$$

Higher heating value of fuel can be determined using heating values and mass shares of constituent elements (fuel ultimate analysis data is needed):

$$HHV_f = HV_C \cdot \frac{\omega_C}{100\%} + HV_H\frac{\omega_H}{100\%} + HV_S\frac{\omega_S}{100\%} + r\frac{\omega_{H_2O}}{100\%}. \tag{5.20}$$

Taking into account data represented in tab. 8, higher heating value of sawdust can be defined as:

$$HHV_{sawdust} = HV_C \cdot \frac{\omega_C}{100\%} + HV_H\frac{\omega_H}{100\%} + HV_S\frac{\omega_S}{100\%} + r\frac{\omega_{H_2O}}{100\%} =$$
$$= 32.8\frac{MJ}{kg}\cdot\frac{32.06\%}{100\%} + 141.8\frac{MJ}{kg}\cdot\frac{0.34\%}{100\%} + 9.16\frac{MJ}{kg}\cdot\frac{0.01\%}{100\%} +$$
$$+2.5\frac{MJ}{kg}\cdot\frac{34.93 + 3.52\cdot 9}{100\%} = 10.52 + 0.48 + 0.001 + 1.67 = 12.6\ \frac{MJ}{kg}.$$

As follows from the proportion proposed above, share of hydrogen taking part in the reaction with 28.19% of fuel oxygen ω_H = 3.52%, so the amount of hydrogen for direct combustion in the furnace is 0.34%.

$$LHV_{sawdust} = HHV_{sawdust} - r\frac{\omega_w + 9\omega_H}{100\%} = 12.6\ \frac{MJ}{kg} - 2.5\frac{MJ}{kg} \cdot 0.67 =$$

$$= 10.93\frac{MJ}{kg}.$$

Fuel combustion process is principally characterized by air amount required for combustion of 1 kg of fuel. For calculation of specific consumption of air basic equations of oxidation can be used:

$C + O_2 \rightarrow CO_2$ (1 $mole\ of\ O_2\ for\ combustion\ of$ 1 $mole\ of\ C$)
$N_2 + O_2 \rightarrow 2NO$ (1 $mole\ of\ O_2\ for\ combustion\ of$ 1 $mole\ of\ N_2$)
$S + O_2 \rightarrow SO_2$ (1 $mole\ of\ O_2\ for\ combustion\ of$ 1 $mole\ of\ S$)
$2H_2 + O_2 \rightarrow 2H_2O$ (1 $mole\ of\ O_2\ for\ combustion\ of$ 2 $mole\ of\ H_2$)

1 m^3 of air contains 21% O_2, 78% N_2 and 1% of other gases. Molar mass of air is 28.98 g/mole. Taking this into account, the amount of air for combustion of 1 kg of fuel can be found from the ratios:

$$n'_a = \frac{\sum n_{O_2}}{21\%} \cdot 100\% = 1000g \cdot \frac{\frac{\omega_C}{M_C} + \frac{\omega_{N_2}}{M_{N_2}} + \frac{\omega_S}{M_S} + 0.5\frac{\omega_{H_2}}{M_{H_2}}}{21\%} \cdot 100\%, \qquad (5.21)$$

$$m'_a = n'_a M_a. \qquad (5.22)$$

Thus, in case of sawdust combustion:

$$n'_a = \frac{\sum n_{O_2}}{21\%} = \frac{26.72m + 0.85m + 0.093m + 0.003m}{21\%} \cdot 100\% =$$

$$= 131.7\ \frac{mole}{1\ kg\ of\ fuel}$$

$$m'_a = n'_a M_a = 131.74\ \frac{mole}{1\ kg\ of\ fuel} \cdot 28.98\frac{g}{mole} = 3.82\ \frac{kg}{1\ kg\ of\ fuel}.$$

3.82 kg of air is required for combustion of 1 kg of sawdust (in theory). 20–30% air excess provides effective combustion in BFB boilers.

Tab. 9. Ultimate sawdust analysis and ratios needed for calculation of air amount.

	Ultimate analysis, %	**Mass share, g/kg of fuel**	**Molar mass, g/mole**	**Mole per 1 kg of fuel**	**Mole of O_2 for comb.**
Carbon	32.06	320.6	12	26.72	26.72
Hydrogen	0.34	3.4	2	1.7	0.85
Oxygen	0	0	32	0	0
Nitrogen	0.26	2.6	28	0.093	0.093
Sulphur	0.01	0.1	32	0.003	0.003
Moisture (H_2O)	66.61	666.1	18	37.01	-
Ash	0.69	6.9	-	-	-

Since the share of sulphur in fuel is known, it is possible to calculate the amount of sorbent (limestone $CaCO_3$). Sorbent binds sulphur oxides (especially toxic sulphur dioxide SO_2) to calcium sulfate:

$$CaCO_3 \rightarrow CaO + CO_2$$
$$CaO + SO_2 + 0.5O_2 \rightarrow CaSO_4$$

Thus, using special nomograms it can be defined that SO_2 removal efficiency at bed temperature 850°C and Ca/S = 3 is around 85% **[19]**. The sorbent amount per 1 kg of fuel can be found from the following equations:

$$m'_{Ca} = 3\omega_S, \tag{5.23}$$
$$m'_s = m'_{Ca} \cdot \frac{M_s}{M_{Ca}}. \tag{5.24}$$

In numerical values:

$$m'_{Ca} = 3\omega_S = 3 \cdot \frac{0.01\%}{100\%} \cdot \frac{1}{1 kg\ of\ fuel} = 0.3 \frac{g\ of\ Ca}{1\ kg\ of\ fuel}.$$

$$m'_s = m'_a \cdot \frac{M_s}{M_{Ca}} = 0.3 \frac{g\ of\ Ca}{1\ kg\ of\ fuel} \cdot \frac{1 \cdot 40\frac{g}{m} + 1 \cdot 12\frac{g}{m} + 3 \cdot 16\frac{g}{m}}{40\frac{g}{m}} =$$

$$= 0.75\ \frac{g\ of\ sorbent}{1\ kg\ of\ fuel}.$$

Sawdust is characterized by low sulphur content and emissions of sulphur oxides during the combustion process are also very low.

5.6. Computational model.

For modeling of temperature regimes inside the furnace of bubbling fluidized bed boiler well-known method of zonal computation is used. Essence of the method is in separation of the total furnace volume into a number of parts (control volumes). Energy balance for each control volume allows to determine the outlet temperature and density of heat flux to the furnace walls. Energy balance includes energy coming from the previous control volume (or from any adjacent volume in case with radiant heat flux), amount of heat released during partial fuel combustion in the present volume, heat with combustion air (for zones of secondary and tertiary air feed) and energy output. Bed temperature in this case is used as a boundary condition for starting calculation.

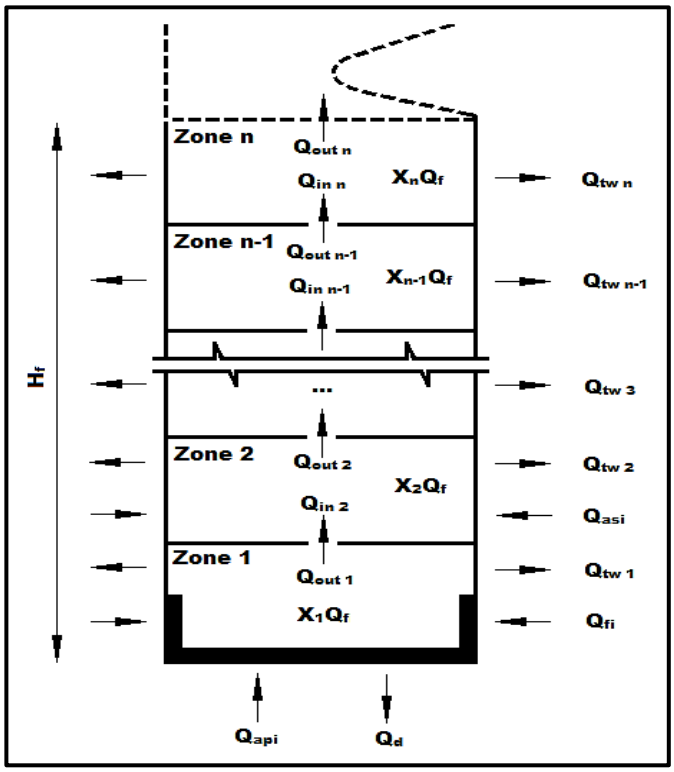

Fig. 13. Scheme of boiler furnace as a series of zones.

One of the main aspects of temperature regimes modeling is associated with combustion fraction profile, a curve indicating the percentage of fuel burning along the furnace height. With a high degree of accuracy, it is possible to assume that combustion fraction profile coincides with heat release profile along the furnace height and in this case it can be described by the function **[20], [25]**:

$$f(h) = e^{-\lambda h} - e^{-\mu h}, \tag{5.25}$$

where the coefficients λ and μ are based on the experience of a specific fuel combustion. Thus, for sawdust it may be used λ=0.6 and μ=1. The obtained dependence for the case under consideration with furnace height 20m is shown on fig. 14. It allows to determine the combustion fraction value in each control volume of the furnace. As can be seen from the graph, combustion fraction in the furnace bed (1 m height) is about 35%. Thus value changes in dependence of fixed/volatile carbon ratio variation.

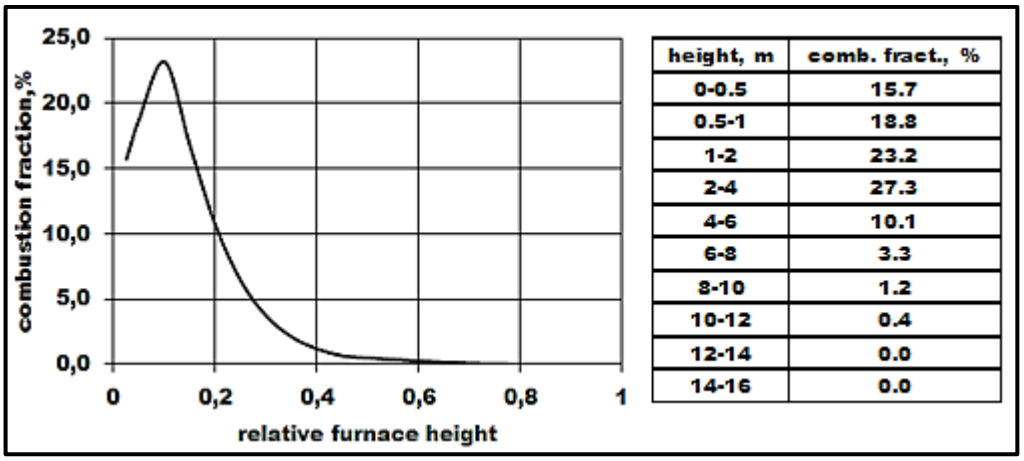

height, m	comb. fract., %
0-0.5	15.7
0.5-1	18.8
1-2	23.2
2-4	27.3
4-6	10.1
6-8	3.3
8-10	1.2
10-12	0.4
12-14	0.0
14-16	0.0

Fig. 14. Combustion fraction profile.

5.7. Case studies and discussion of results.

As it was mentioned above, the present model is based on the real BFB boiler in Kuusankoski, Finland. Input data for case studies is indicated in tab. 10. Thus,

examination of 1–5 cases allows to determine the influence of bed material fineness on temperature distribution inside the boiler furnace. Profiles of heat flux and heat transfer coefficient for each case give more detailed explanation of internal heat transfer processes. Cases 5–7 are examined for estimation of air excess effect on furnace temperature conditions. The third group of cases (5, 8, 9) aims to define the temperature regime in dependence on boiler heat load.

Tab. 10. Parameters used for modeling of different regimes.

Case	Particle size, mm	Air excess coef.	Boiler load coef.
1	0.1	1.25	1
2	0.15	1.25	1
3	0.2	1.25	1
4	0.25	1.25	1
5	1	1.25	1
6	1	1.3	1
7	1	1.4	1
8	1	1.25	0.8
9	1	1.25	0.6

Size of bed material particles (fineness) is one of the main characteristics of fluidized bed. Obtained mean temperature distribution along relative furnace height (fig. 15) shows the influence of particle size on a thermal regime in the furnace of BFB boiler. Principle trand is that inside the furnace with fluidized bed formed by coarse particles mean temperature is higher than in case of beds from fine material. It can be explained by the following reason. At the similar superficial velocities voidage of fluidzed bed from fine particles is higher, bubbling process is more intensive and more single particles and clusters are entrained to the freeboard. In cases with fine particles bed height can reach refractory height or even surpass it. Due to the contact between water wall tubes and particles the efficiency of heat transfer process rises and more heat can be absorbed by tube surface. It leads to reduction of local temperature and mean furnace temperature as well.

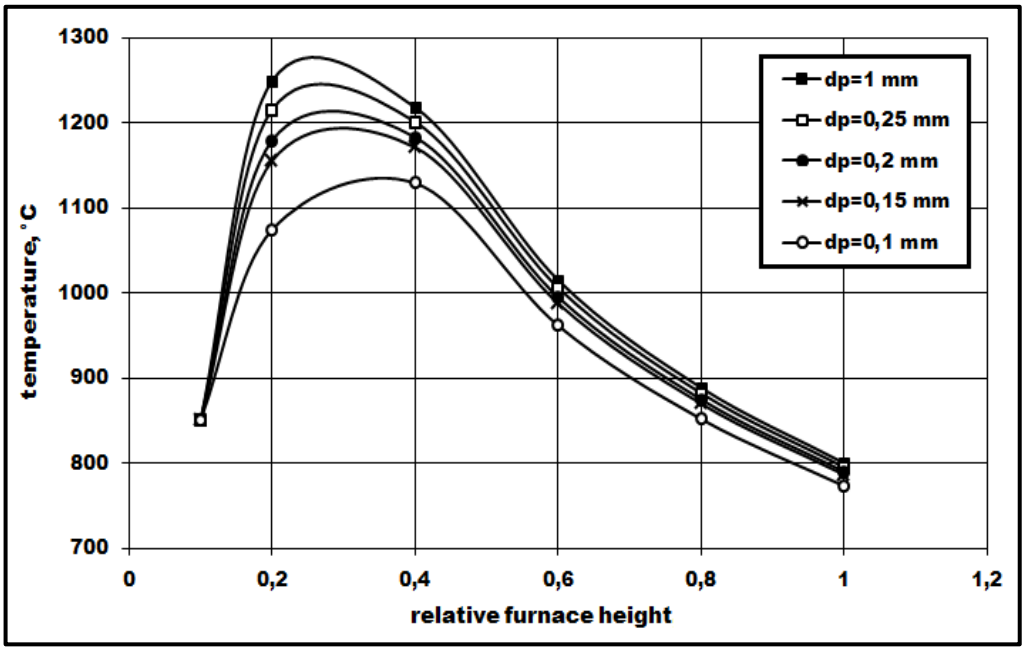

Fig. 15. Effect of bed material fineness on a temperature profile (cases 1–5).

Tab. 11. Numerical values of temperature (cases 1–5).

	Temperature according to relative furnace height, °C					
d_p, mm	0.1	0.2	0.4	0.6	0.8	1.0
1	850	1249	1218	1015	888.5	800
0.25	850	1215	1201	1006	882	795.2
0.2	850	1179	1183	995	874.7	789.9
0.15	850	1155	1171	987.7	869.7	786.3
0.1	850	1074	1129	961.6	851.8	773

As also follows from the graph, maximum temperature in the furnace is achieved above the surface of the fluidized bed in the zone of volatiles combustion. For fuels with high volatile/fixed carbon ratio as in this case, combustion process occurs mainly in the freeboard, while high fixed carbon content shifts it to the surface of fluidized bed.

Fig. 16 indicates change of convective component of total heat transfer coefficient from the bed surface level to the furnace exit. It is evident from the graph that with particle diameter decrease heat transfer coefficient rises as small particles have more contact points per unit of tube surface in comparison with

large particles. Exponential character of heat transfer coefficient shows its relation with voidage fraction and emulsion density. Thus, it decreases sharply from the level of fluidized bed surface as emulsion phase density does.

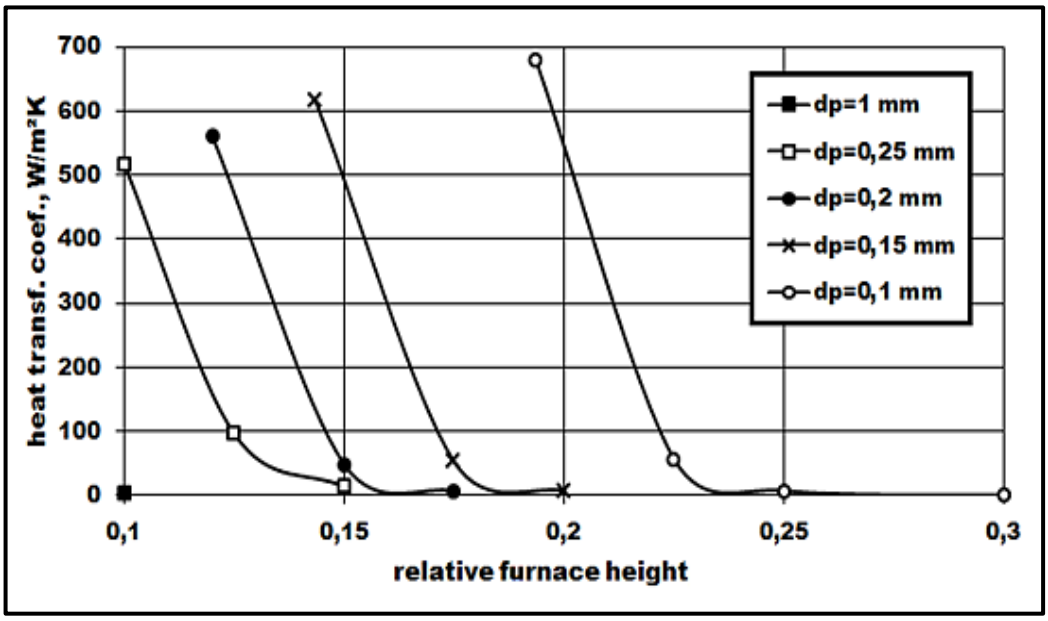

Fig. 16. Effect of bed material fineness on a convective component of heat transfer coefficient (cases 1–5).

Tab. 12. Numerical values of convective heat transfer coefficient (cases 1–5).

	Convective heat transfer coefficient according to relative furnace height, W/m^2·K					
d_p, mm	0.1	0.15	0.175	0.2	0.25	0.3
1	4.5	0.06	0.009	0	0	0
0.25	517	13.2	1.77	0.237	0	0
0.2	561.1	48.5	6.6	0.89	0	0
0.15	615.6	383.2	52.4	6.96	0.9	0.16
0.1	680.7	680.7	680.7	520.8	7.52	0.137

Change of heat flux to the walls in dependence of particle size is shown on fig. 17. It is to be noted that in the lower zone of furnace heat flux is considerably higher in case with fine bed particles while in the middle and upper zones the value of heat flux is higher for cases with particles of larger diameter. It correlates with

temperature and heat transfer coefficient profiles obtained for each case. Particle convection noticeably increases total heat transfer coefficient at high values of solids concentration near tube walls (as in case with fine particles). It provides considerable rise of heat flux value. Absorption of large amount of heat by tube walls in the lower zone of furnace explains the lower mean furnace temperature in comparison with case when coarse bed material is used. When concentration of solids in the furnace space decays to zero radiation becomes the only mechanism of heat transfer (gas convection at low velocities is negligible). In case when mean furnace temperature is higher (coarse bed material) heat transfer coefficient is also higher and process of heat transfer is more intense as confirmed by heat flux profiles (fig. 17).

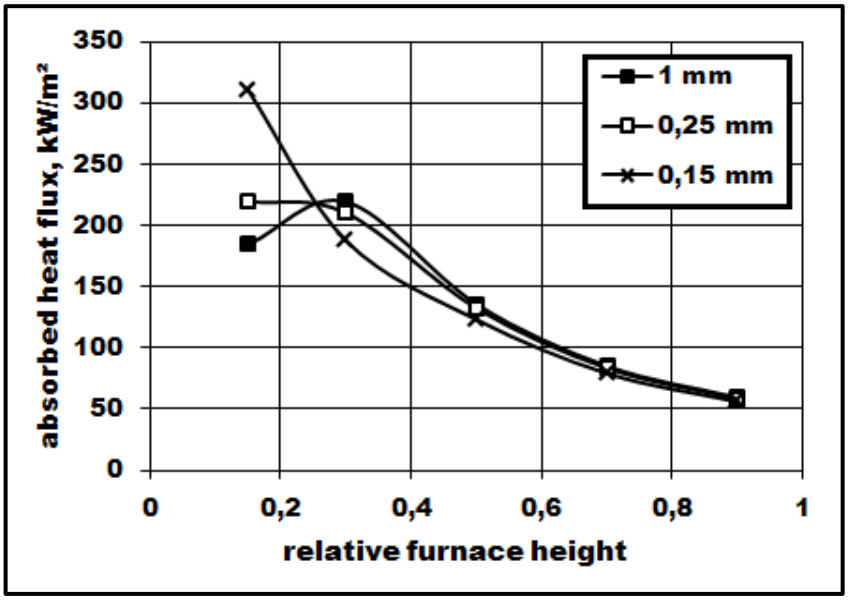

Fig. 17. Effect of bed material fineness on a heat flux absorbed by water tube walls (cases 2, 4, 5).

Tab. 13. Numerical values of specific heat flux to the furnace walls (cases 2, 4, 5).

	Specific heat flux according to relative furnace height, kW/m^2				
d_p, mm	0.15	0.3	0.5	0.7	0.9
1	184.27	219.21	135.68	85.10	59.36
0.25	219.56	210.13	132.16	83.43	58.15
0.15	310.48	187.40	123.02	79.06	55.95

As also can be seen from the graph, intensive heat release during volatiles combustion in the zone above fluidized bed only slightly retards the rate of heat flux reduction in case of fine bed material, while in case when coarse particles are used the value of heat flux increases.

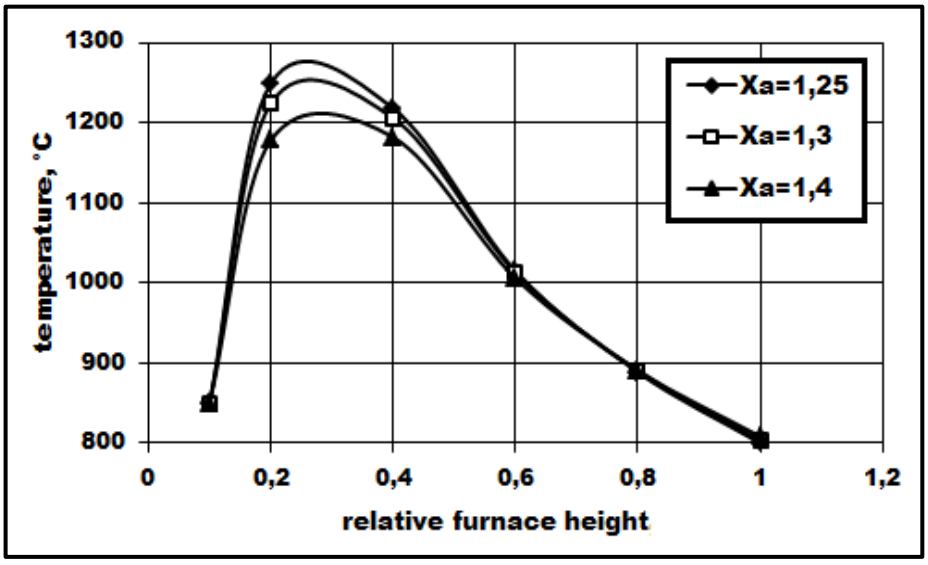

Fig. 18. Effect of air excess on a temperature profile (cases 5–7).

Excess air ratio has influence on a number of boiler operational parameter. Efficiency of combustion process initially increases with increase of excess air ratio and after certain moment starts to decrease. The value of air excess is based on the experience of specific fuel combustion. Intensive heat transfer and constant mixing make the process of bubbling fluidized bed combustion effective at low (1.2–1.3) excess air ratio **[14]**. Together with staged air feeding it provides low NO_x emissions.

As evident from fig. 18 maximum temperature in the furnace becomes lower with increase of excess air ratio. Even if it slightly improves the efficiency of fuel combustion, heat losses with increased flue gases flow and mean furnace temperature reduction make the total efficiency lower.

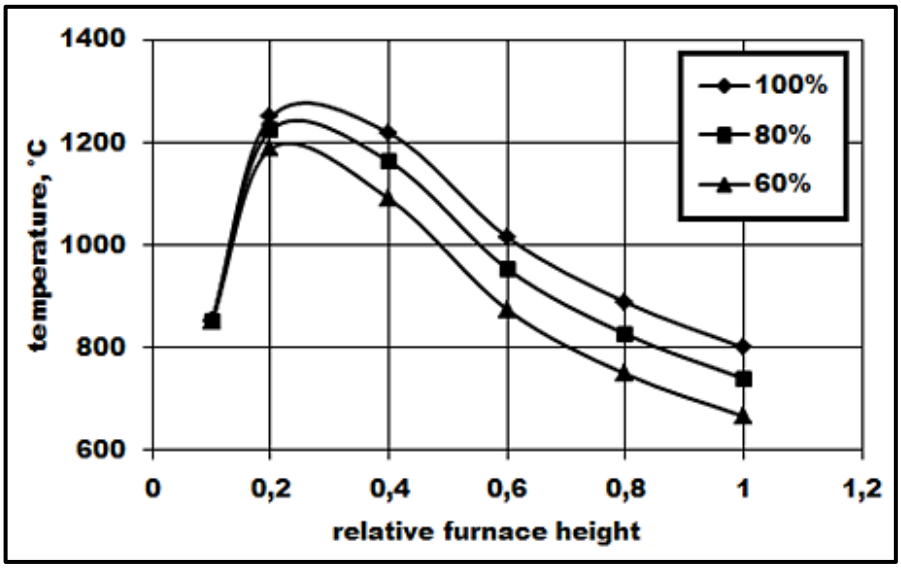

Fig. 19. Effect of boiler load on a temperature profile (cases 5, 8, 9).

The influence of boiler load on temperature profile is represented on fig. 19. Thus, decrease in fuel feed leads to reduction of maximum furnace temperature and in a greater extent to reduction of exit temperature.

The accuracy of zonal temperature calculation depends on the chosen number of zones. Taking into account a number of simplifications used throughout the process of model creation, the accuracy of the calculations is not very high. Nevertheless, model can be applied for qualitative assessment of temperature distribution inside the furnace and for estimation of influence of different parameters on it.

6. CONCLUSION.

A number of global problems such as growing energy consumption and reduction of fossil fuel reserves lead to development of new technologies of energy production. High level of carbon dioxide emission turns the attention to ecological aspects of these technologies.

Bioenergy plays a significant role in solving the problems stated above. The potential of biofuel utilization is huge. In the last years, share of biofuels in the global energy production has increased greatly. It promotes the development and modernization of biofuel combustion technologies.

One of the most effective and commonly used technologies – combustion in bubbling fluidized bed – was under consideration in this project.

The main aim of the project was to create a simplified one-dimensional model of bubbling fluidized bed boiler for qualitative assessment of temperature distribution inside the furnace in dependence on different parameters. Thus, effects of bed material fineness, excess air ratio and changes in boiler load were studied. Case studies give a fairly complete idea of heat exchange processes inside the furnace and allow to estimate influence of definite factors on thermal regime. Securing of a proper thermal regime during fuel combustion has a direct influence on the efficiency of energy production.

REFERENCES

1. International Energy Agency statistics, 2011. World: Electricity and heat. http://www.iea.org/statistics/statisticssearch/report/?country=WORLD&product=electricityandheat&year=2011
2. **Basu, Prabir. 2006.** *Combustion and gasification in fluidized beds.* Boca Raton, FL: CRC Press/Taylor & Francis Group, 2006.
3. **Oka, Simeon; Anthony, E. J.. 2004.** *Fluidized bed combustion*. New York: M. Dekker, 2004.
4. **Spliethoff, Hartmut. 2010.** *Power generation from solid fuels.* Berlin Heidelberg: Springer-Verlag, 2010.
5. **The World Coal Institute.** *Clean coal – building a future through technology*. Economic commission for Europe committee on sustainable energy, Ad Hoc Group of Experts on Coal in Sustainable Development. Seventh session, 2004.
6. **Pena, J. A..** *Bubbling fluidized bed. When to use this technology?* Foster Wheeler Global Power Group, Madrid, Spain. Industrial Fluidization South Africa, Johannesburg, 2011.
7. **Bowman, J.; Davidson, M.; Penterson, J.; Toupin, K..** *Biomass combustion technologies: a comparison of a biomass 50MW modern stoker fired system and a bubbling fluidized bed system.* Riley Power Inc., 2010.
8. **Ryabov, Georgy; Litoun, Dmitry; Dik, Eduard.** *Agglomeration of bed material: influence on efficiency of biofuel fluidized bed boiler.* Thermal Science, vol. 7, issue 1, pp. 5–16, 2003.
9. International Energy Agency statistics, 2008. Total World Electricity Generation by Fuel.
10. **Gaur, Siddhartha.** *Thermal data for natural and synthetic fuels.* CRC Press, 1998.
11. **Tillman, David; Duong, Dao.** *Solid fuel blending: principles, practices, and problems.* Butterworth-Heinemann, 2012.

12. Biomass Energy Centre: Carbon emissions of different fuels. http://www.biomassenergycentre.org.uk/portal/page?_pageid=75,163182&_dad=portal&_schema=PORTAL
13. Specific Carbon Dioxide Emissions of Various Fuels, online data service. http://www.volker-quaschning.de/datserv/CO2-spez/index_e.php
14. **Koppejan, Jaap; Van Loo, Sjaak.** *The handbook of biomass combustion and co-firing.* Earthscan Publications Ltd., 2008.
15. **Siemons, Roland.** *The mechanism of char ignition in fluidized bed combustors.* Combustion and flame journal 70, pp. 191–206, 1987.
16. **Grace, J. R..** *Fluid beds as chemical reactors*. In *Gas fluidization technology*, Geldart, D.. Wiley, 1986.
17. **Wen, C. Y.; Chen L. H..** *Fluidized bed freeboard phenomena and elutriation.* AIChE journal 1, pp. 117–128, 1982.
18. **Andersson, B. A..** *Heat transfer in stationary fluidized bed boilers.* Ph. D. dissertation, Chalmers University of Technology. Goteborg, 1988.
19. **Zevenhoven, Ron; Kilpinen, Pia.** *Control of pollutants in flue gases and fuel gases.* On-line book: http://users.abo.fi/rzevenho/gasbook.html
20. **Blokh, A. G..** *Heat transfer in steam boiler furnaces.* Washington, D.C: Hemisphere, 1988.
21. **Singer, E..** *Combustion – fossil power systems.* Windsor: Combustion Engineering, Inc., 1981.
22. DIN 17175 Seamless tubes of heat resistant steels, 1979.
23. **Baukal, Charles.** *Heat transfer in industrial combustion.* Boca Raton, FL: CRC Press, 2000.
24. **Gomez-Barea, A.; Leckner, B..** *Modeling of biomass gasification in fluidized bed.* Progress in energy and combustion science journal 36, pp. 444–509, 2010.
25. **Kouprianov, V..** *Modeling of thermal characteristics for a furnace of a 500 MW boiler fired with high-ash coal.* Energy 26, pp. 839–853, 2001.
26. **Quaak, Peter; Knoef, Harrie; Stassen, Hubert.** *Energy from biomass: a review of combustion and gasification.* World Bank Publications, 1999.

27. **Yang, Wen-Ching.** *Handbook of fluidization and fluid-particle systems.* Taylor & Francis Group LLC, 2003.

28. **DeFusco, J. P.; Mckenzie, P.A.; Fick, M.D..** *Bubbling fluidized bed or stoker – which is the right choice for your renewable energy project?* The Babcock and Wilcox Company. CIBO fluid bed combustion 20th conference, Lexington Kentucky, 2007.

29. **Aguas, M.; Azevedo, J.; Carvalho, M..** *Modelling the heat transfer in a fluidized bed combustor.* Heat and technology journal, vol. 10, issue 1–2, pp. 107–124, 1992.

30. **Molerus, O., Wirth, K..** *Heat transfer in fluidized beds.* London: Chapman and Hall, 1997.